学位論文

Studies on processing and function of CLE peptides in *Arabidopsis thaliana*.

（シロイヌナズナにおける CLE ペプチド
の プロセシングと機能の研究）

平成 25 年 12 月博士(理学)申請

東京大学大学院理学系研究科
生物科学専攻

玉置　貴之

Contents

Acknowledgements

I would like to express my deepest thanks to Dr. Hiroo Fukuda and Dr. Shinichiro Sawa for supervising my research. I am also very grateful to Dr. Shigeyuki Betsuyaku for good advise in biochemical experiments, Dr. Masayuki Fujiwara and Dr. Yoichiro Fukao for collaboration in MS analyses, and Dr. Yoshihisa Oda for instructions in experiments using *Arabidopsis* cell cultures. I also appreciate Yukiko Sugisawa for help with microarray analyses. All members of Fukuda laboratory and my family supported many things and I would like to express again my thanks to them. I thank David Baulcombe (Department of Plant Sciences, University of Cambridge) and Plant Bioscience Ltd (www.pbltechnology.com) for the *Rhizobium radiobacter* (*Agrobacterium tumefaciens*) strain carrying the p19 silencing suppressor, Jane Parker (Department of Plant Microbe Interactions, Max Planck Institute for Plant Breeding Research) for pXCSG-3HS, Tsuyoshi Nakagawa (Department of Molecular and Functional Genomics, Center for Integrated Research in Science, Shimane University) for the pGWB1, R4pGWB401 and R4pGWB433 binary vectors, Ueli Grossniklaus (Institute of Plant Biology and Zürich-Basel Plant Science Center, University of Zürich) for pMDC7, Takashi Ueda for valuable discussions and support with the confocal microscopic observations, Kazuo Ebine for support with the confocal microscopic observations and for the *35S:TagRFP-ARA7* construct, Emi Ito for the *35S:TagRFP-ARA7* construct, Ikuko Hara-Nishimura (Department of Botany, Graduate School of Science, Kyoto University) for the *35S:SP-GFP-HDEL* construct, Keiko

Shoda (Molecular Membrane Biology Laboratory, RIKEN Advanced Science Institute) for the *35S:ST-mRFP* construct, Tomohiro Uemura for the *35S:mRFP-SYP61* construct and Rie Kurata (Plant Global Education Project, Graduate School of Biological Sciences, Nara Institute of Science and Technology) for help with the mass spectrometric analysis. Contents of chapter 1 were published in *The Plant Journal* as an original article entitled "SUPPRESSOR OF LLP1 1-mediated C–terminal processing is critical for CLE19 peptide activity" (Tamaki *et al.* (2013) *The Plant Journal.* 76, 970–981).

List of Abbreviations

35S	35S promoter of cauliflower mosaic virus
ºC	degree Celsius
AG	AGAMOUS
Ala	Alanine
Arg	Arginine
ARR7	ARABIDOPSIS RESPONSE REGULATOR 7
bp	base pair(s)
C-terminal	carboxy-terminal
cDNA	complementary DNA
ChIP-Seq	Chromatin Immunoprecipitation Sequencing
CLE	CLAVATA3/EMBRYO-SURROUNDING REGION-RELATED
CLV1	CLAVATA1
CLV2	CLAVATA2
CLV3	CLAVATA3
cm	centimeter
Col-0	Columbia-0
CPD	carboxypeptidase D
CPE	carboxypeptidase E
Dansyl	Dansyl groop
DOF2	DOF ZINC FINGER PROTEIN 2

DMSO	dimethylsulfoxide
DNA	deoxyribonucleic acid
DNase	deoxyribonuclease
ECFP	Enhanced Cyan Fluorescent Protein
EDTA	ethylenediaminetetraacetic acid
ER	Endoplasmic Reticulum
ER	ERECTA
ERF4	ETHYLENE RESPONSIVE ELEMENT BINDING FACTOR 4
ERF12	ERF DOMAIN PROTEIN 12
ERT2	ETHYLENE-RESPONSIVE NUCLEAR PROTEIN/ETHYLENE-REGULATED NUCLEAR PROTEIN 2
EtOH	ethanol
g	gram
g	gravity constant (9.81 ms^{-2})
GFP	Green Fluorescent Protein
GUS	β-glucuronidase
h	hours
HA	hemagglutinin of influenza virus
HB-2	HOMEOBOX PROTEIN 2
HB40	HOMEOBOX PROTEIN 40
HCl	hydrochloric acid
IAA31	INDOLE-3-ACETIC ACID INDUCIBLE 31

IgG-HRP	Immunoglobulin G conjugated to horseradish peroxidase
K	Lysine in the context of amino-acid sequence
kbp	kilo base pairs
l	liter
LLP1	LIGAND LIKE PROTEIN 1
LRR-RLK	Leucine-Rich Repeat Receptor-Like kinase
µ	micro
µg	microgram
µl	microliter
µM	micromolar
µm	micrometer
M	molar
MALDI-TOF	Matrix-Assisted Laser Desorption IonizationTime-Of-Flight Mass Spectrometry
MES	2-morpholinoethanesulfonic acid
mg	milligram
min	minute(s)
MIR165A	MICRORNA165A
ml	milliliter
mM	millimolar
mRFP	monomeric red fluorescent protein
MS medium	Murashige and Skoog medium

nM	nanomolar
N-terminal	NH_2-terminal
PCR	Polymerase Chain Reaction
pg	picogram
pH	negative decimal logarithm of the H^+ concentration
Phe	Phenylalanine
PRS	PRESSED FLOWER
qRT-PCR	Quantitative Reverse Transcription Polymerase Chain Reaction
R	Arginine in the context of amino-acid sequence
RAM	Root Apical Meristem
RNA	ribonucleic acid
RNase	ribonuclease
RPK2	RECEPTOR-LIKE PROTEIN KINASE 2
rpm	rounds per minute
SAM	shoot apical meristem
sec	second(s)
SOL1	SUPPRESSOR OF LLP1 1
SOL1-3HS	SOL1 C-terminally fused to a triple HA/single StrepII tag
SYP61	SYNTAXIN OF PLANTS 61
TagRFP	Tag Red Fluorescent Protein
TDIF	Tracheary Element Differentiation Inhibitory Factor
T-DNA	transfer DNA

TDR	TDIF RECEPTOR
TFA	Trifluoroacetic acid
TPL	*TOPLESS*
TPR1	*TOPLESS-RELATED 1*
TPR2	*TOPLESS-RELATED 2*
Tris	tris-(hydroxymethyl)-aminomethane
TUA4	TUBULIN ALPHA-4 CHAIN
v/v	volume per volume
VND6	VASCULAR-RELATED NAC-DOMAIN 6
w/v	weight per volume
WOX	WUSCHEL-RELATED HOMEOBOX
WUS	WUSCHEL
YFP	yellow fluorescent protein

Abstract

Intercellular communications mediated by members of the CLAVATA3/EMBRYO-SURROUNDING REGION-RELATED (CLE) family, a group of small secretory peptides, have important roles in plant development such as stem cell maintenance in plant meristems. CLE signals are commonly transduced through their receptors, Leucine-Rich Repeat Receptor-Like Kinases (LRR-RLKs), to WUSCHEL (WUS)-RELATED HOMEOBOX (WOX) transcription factors promoting stem cell proliferation. However, many problems such as maturation mechanism of CLE peptides, signal transduction from LRR-RLK to WOX transcription factor, WOX dependent regulation of downstream genes, crosstalk with other signaling pathways, still remain to be solved. In this study, to uncover overall CLE functions, I performed analyses on processing mechanisms of CLE peptides and downstream signaling of CLE peptides mediated by *WOX* genes.

I first demonstrated that SUPPRESSOR OF LLP1 1 (SOL1), a putative Zn^{2+} carboxypeptidase, functions in C-terminal processing of the CLE19 proprotein. SOL1 showed enzymatic activity to remove the C-terminal arginine or lysine residue of CLE19, CLE21, CLE22 proproteins *in vitro*, and SOL1-dependent cleavage of the C-terminal arginine is essential for CLE19 activity *in vivo*. The localization analysis of SOL1 indicated its endosomal localization, which suggests that this processing occurs in endosomes in the secretory pathway.

Secondly, to decipher WOX functions as downstream transcription factors of CLE peptides, I investigated downstream genes of WOX4 and WUS. For this purpose, transgenic *Arabidopsis* cell cultures expressing estrogen-inducible *WOX4-ECFP* and *WUS-ECFP* were produced. Microarray analysis revealed that *WOX4-ECFP* and *WUS-ECFP* expression rapidly changed gene expression profiles of these cells, supporting an assumption that WOX4-ECFP and WUS-ECFP are functional as transcription factors even in this system. WOX4-ECFP-induced genes were largely different from WUS-ECFP-induced genes, implying distinct function between WOX4 and WUS. These data raise posttranslational processing as a critical step for regulating CLE activities and also provide useful information for further studying downstream factors of CLE signaling. Thus, these data shed light on as yet unknown mechanisms controlling CLE functions.

Chapter I: General introduction

Multicellular organisms utilize intercellular communication to coordinate cellular differentiation and proliferation precisely, thus achieving organized development. In plants, phytohormones, such as auxin and cytokinin, are known to function as intercellular signaling molecules (Moubayidin *et al.*, 2009). In addition to these conventional phytohormones, small secretory peptides have also been implicated as important factors that mediate cell-to-cell signaling. There are two groups of small secretory peptides in plants, cysteine-rich peptides and small post-translationally modified peptides (Matsubayashi, 2011). Cysteine-rich peptides are distinctive for harboring even number of cysteine residues involved in formation of intramolecular disulfide bonds (Pearce *et al.*, 2001; Okuda *et al.*, 2009; Kondo *et al.*, 2010). Small post-translationally modified peptides are characterized by post-translational modification and proteolytic processing to produce functional small mature peptides (Ohyama *et al.*, 2008; Srivastava *et al.*, 2008; Srivastava *et al.*, 2009; Matsuzaki *et al.*, 2010).

Amongst small post-translationally modified peptides, the CLAVATA3 /EMBRYO-SURROUNDING REGION-RELATED (CLE) peptides have been extensively studied because of their various important functions in plant development and plant-microbe interactions (Hirakawa *et al.*, 2008; Miwa *et al.*, 2008; Müller *et al.*, 2008; Stahl *et al.*, 2009; Bleckmann *et al.*, 2010; Hirakawa *et al.*, 2010; Kinoshita *et al.*, 2010; Kiyohara and Sawa, 2012; Yamada and Sawa, 2013). The CLE peptides regulate

differentiation and proliferation of stem cells in the shoot apical meristem (SAM), the vascular meristem and the root apical meristem (RAM). The CLE signaling pathway is composed of a CLE peptide, Leucine-Rich Repeat Receptor-Like Kinases (LRR-RLKs) as receptors and a WUSCHEL-RELATED HOMEOBOX (WOX) transcription factor.

In *Arabidopsis thaliana*, 32 *CLE* genes exist in the genome and are expressed in various tissues (Oelkers *et al.*, 2008; Jun *et al.*, 2010). These genes encode proproteins comprising approximately 100 amino acid residues, which carry an N-terminal signal peptide, the conserved 14 amino acid C-terminal CLE domain, and a less conserved variable domain between them (Cock and McCormick, 2001; Rojo *et al.*, 2002). Genetic and physiological studies raised CLAVATA1 (CLV1), TDIF RECEPTOR (TDR) and ACR4 as receptors of CLE peptides (Hirakawa *et al.*, 2008; Ogawa *et al.*, 2008; Stahl *et al.*, 2009). They belong to LRR-RLK family and there are over 230 LRR-RLKs in *A. thaliana* and are characterized by extracellular LRR domain, involved in ligand binding, transmembrane domain and intracellular kinase domain involved in downstream signaling (Ogawa *et al.*, 2008; Wang *et al.*, 2008). As downstream factors of the CLE-LRR-RLK signaling pathways, *WUSCHEL* (*WUS*), *WOX4* and *WOX5* promote stem cell proliferation in the shoot apical meristem, the vascular meristem and the root apical meristem, respectively (Stahl *et al.*, 2009; Hirakawa *et al.*, 2010; Yadav *et al.*, 2010). *WOX* genes encode homeodomain transcription factors and are considered to function through transcriptional regulation of their target genes.

The outline of CLE peptide regulation has been understood. However, there are still many unsolved important issues about CLE signaling such as maturation

mechanism of CLE peptides, signal transduction from LRR-RLK to WOX transcription factor, WOX dependent regulation of downstream genes, crosstalk with other signaling pathways, etc. Toward understanding the whole process of the CLE signaling, in this study, I attempted to elucidate two important problems, that is, maturation process of CLE peptides and downstream signaling of WOX transcription factors among a number of problems. In chapter 1, I performed detailed analysis on a Zn^{2+} carboxypeptidase, SUPPRESSOR OF LLP1 1 (SOL1), in relation to CLE processing. In chapter 2, I investigated downstream genes of WOX4 and WUS using microarray.

Chapter II: Materials and methods

Plant materials and growth conditions

Columbia-0 (Col-0), *sol1-101* (SALK_13659c), *sol1-102* (SALK_15449c), *rpk2-2* (Mizuno *et al.*, 2007; Kinoshita *et al.*, 2010), *clv1-101* (Kinoshita *et al.*, 2010), *clv3-8 ER* (CS3604), *at1g28360* (CS877578), *at3g15210* (SALK_073394C), *at4g20880* (SALK_005550C) and *iaa31-1* (CS25218) seeds were obtained from the Arabidopsis Biological Resource Center (www.abrc.osu.edu) at Ohio State University (Diévart *et al.*, 2003). *clv2-101* (GK686A09), *wox4-1* (GABI462G01), *at1g01183* (GK089D01) and *at5g64800* (GK203E06) seeds were obtained from GABI-Kat (www.gabi-kat.de, Kleinboelting *et al.*, 2012). All lines used in this study are in the Col-0 background, except for *clv3-8* (unknown background) and *clv1-101* (Col-2 background).

For carpel number analysis, seeds, which had been incubated in water at 4°C for 2 days, were sown on soil and grown at 22°C under continuous white light (20-50 μmol m^{-2} sec^{-1}). For root length assays, GUS histochemical analysis, *SOL1* expression analysis and hypoctyl section assays, surface-sterilized seeds were plated on growth medium containing 0.23% (w/v) Murashige and Skoog basal salts, 1% (w/v) sucrose, 0.05% (w/v) MES monohydrate (pH 5.7), 0.0005% (w/v) thiamine hydrochloride, 0.0001% (w/v) nicotinic acid, 0.0005% (w/v) pyridoxine hydrochloride, 0.01% (w/v) myo-inositol, 0.002% (w/v) glycine and 1.5% (w/v) agar. For CLE peptide treatment, 1/10000 volume (for MCLV3 and CLE19) or 1/5000 volume (for TDIF) of peptide solutions or 0.1% trifluoroacetic acid was added to the medium. For estrogen-induced

expression, 1/2000 volume of 10 mM β-estradiol dissolved in dimethylsulfoxide (DMSO) or DMSO alone was added. The peptide solutions were dissolved in 0.1% trifluoroacetic acid to concentrations of 10 mM, 5 mM (for TDIF), 1 mM, 100 μM and 10 μM, respectively. Seedlings were grown for 9 days (for root length assay), 12 days (for GUS staining) or 16 days (for expression analysis of *SOL1* and hypocotyl section assays) at 22°C under continuous white light (20-50 μmol m^{-2} sec^{-1}) after a two-day incubation at 4°C. For estrogen-induced expression analysis, surface-sterilized seeds were sown in 9 ml of liquid growth medium containing 0.23% (w/v) Murashige and Skoog basal salts, 1% (w/v) sucrose, 0.05% (w/v) MES monohydrate (pH 5.7), 0.0005% (w/v) thiamine hydrochloride, 0.0001% (w/v) nicotinic acid, 0.0005% (w/v) pyridoxine hydrochloride, 0.01% (w/v) myo-inositol and 0.002% (w/v) glycine, and then grown at 22°C under continuous white light (20-50 μmol m^{-2} sec^{-1}) with shaking at 110 rpm.

Construction of plasmids and transgenic plants

The primers used in Chapter III are listed in Table 2-1, and all the coding sequences used in this study were amplified by PCR from cDNA derived from young Col-0 seedlings. The *SOL1* promoter sequences were amplified from Col-0 genomic DNA. The Gateway Cloning System (Life Technologies, www.lifetechnologies.com/) was used unless stated. The estrogen-inducible *CLV3*, *CLE19* and *CLE19*Δ*R* constructs were generated as follows: PCR amplification products were cloned into pENTR-D/TOPO (for *CLE19*) or pDONR221 (for *CLV3* and *CLE19*Δ*R*), and then cloned through the LR

reaction into pMDC7 (Curtis and Grossniklaus, 2003) in accordance with the manufacturer's instructions for the Gateway Cloning System. A mutated primer was used to cause an arginine codon deletion into *CLE19ΔR*. As for the *SOL1pro:GUS* construct, the 2370 bp sequence upstream of the *SOL1* translational initiation site and the *GUS* coding sequence from R4pGWB433 were amplified independently, fused by PCR, and then cloned into R4pGWB401. The estrogen-inducible *SOL1-3HA-StrepII* (*SOL1-3HS*) and *SOL1-YFP* constructs were generated as follows: the *SOL1* coding sequence without the stop codon was cloned into pXCSG-3HS and pH35GY resulting in pXCSG-SOL1-3HS and pH35GY-SOL1-YFP, respectively. Subsequently, the *SOL1-3HS* and *SOL1-YFP* sequences were amplified from these vectors, and then cloned into pMDC7. *35S:SP-GFP-HDEL*, *35S:ST-mRFP* and *35S:mRFP-SYP61* were provided by I. Hara-Nishimura (Department of Botany, Graduate School of Science, Kyoto University, Japan), K. Shoda (Molecular Membrane Biology Laboratory, RIKEN Advanced Science Institute, Japan) and T. Uemura (Department of Biological Sciences, Graduate School of Science, The University of Tokyo, Japan), respectively. *35S:TagRFP-ARA7* was obtained from E. Ito (Department of Biological Sciences, Graduate School of Science, The University of Tokyo, Japan) and K. Ebine (Department of Biological Sciences, Graduate School of Science, The University of Tokyo, Japan).

The primers used in Chapter IV are listed in Table 2-2. The estrogen-inducible constructs, pER8-CFP and pER8-GW-CFP, were constructed from pER8 as described in previous report (Zuo *et al.*, 2000; Ohashi-Ito *et al.*, 2010). The estrogen-inducible

pER8-WOX4-ECFP and pER8-WUS-ECFP constructs were generated as follows: Coding sequence of *WOX4* and *WUS* were cloned into pENTR-D/TOPO, and then cloned through the LR reaction into pER8-GW-CFP in accordance with the manufacturer's instructions for the Gateway Cloning System (Life Technologies, www.lifetechnologies.com/) (Ohashi-Ito *et al.*, 2010). For construction of $WOX4_{pro}$:*WOX4-ECFP*, genomic fragment of *WOX4* starting from 3 kbp upstream from translational start site to 1.5 kbp downstream from translational stop site was cloned into pENTR-D/TOPO. After removing exon and intron of *WOX4* from resulting plasmid by PCR, *WOX4-ECFP* fragment amplified from pER8-WOX4-CFP was inserted into the plasmid through the In-Fusion HD reaction (TAKARA BIO, www.takara-bio.co.jp). Then, $WOX4_{pro}$:*WOX4-ECFP* in pENTR-D/TOPO backbone was cloned into pGWB1 through the LR reaction (Life Technologies, www.lifetechnologies.com/).

R4pGWB401-SOL1pro:GUS, pMDC7-CLV3, pMDC7-CLE19, pMDC7-CLE19 ΔR and pGWB1-$WOX4_{pro}$:WOX4-ECFP were transformed into *R. radiobacter* strain GV3101::pMP90 and then into Col-0, *sol1-101* or *wox4-1* plants using the floral-dip method (Clough and Bent, 1998). Other plasmids were also transformed into *R. radiobacter* strain GV3101::pMP90 and used for *N. benthamiana* transient expression or producing the transgenic *Arabidopsis* cell cultures.

GUS staining

Plants were incubated in 90% acetone for 15 min on ice, washed with 100 mM

$NaPO_4$ buffer (pH 7.0), vacuum-infiltrated at room temperature for 15 min with GUS staining solution containing 100 mM $NaPO_4$ (pH 7.0), 10 mM EDTA, 1 mM potassium ferrocyanide, 1mM potassium ferricyanide, 0.1% Triton X-100 and 1 mg ml^{-1} 5-Bromo-4-chloro-3-indolyl-D-glucuronide cyclohexylammonium salt, and incubated at 37°C for 6 h. GUS-stained samples were incubated at room temperature in 70% EtOH for 1 h and then in a mixture of EtOH:acetic acid (6:1 v/v) for more than 3 h, and stored in 70% EtOH. Samples were mounted in a mixture of chloral hydrate/glycerol/water (8 g/1 ml/2 ml) for microscopic observation, or embedded in Technovit 7100 resin (Heraeus Kulzer, www.heraeus-kulzer.com/) for sectioning of the shoot apical meristem.

Tissue sectioning

GUS-stained samples stored in 70% EtOH and hypocotyl samples fixed with a mixture of 70% EtOH/acetic acid/formaldehyde (18:1:1 in volume) were dehydrated in a graded ethanol series, and embedded in Technovit 7100 resin (Heraeus Kulzer, www.heraeus-kulzer.com/) according to the manufacturer's instructions. Sections (10 μm or 2 μm thick) were prepared using a Leica RM2165 microtome (www.leica.com) and then mounted in water or stained with 0.05% (w/v) Toluidine Blue O solution for microscopic observation.

Preparation of cDNA for qRT-PCR analysis

Total RNA was extracted from whole seedlings or transgenic *Arabidopsis* cell cultures using TRIzol Reagent (Life Technologies, www.lifetechnologies.com/) according to the manufacturer's instruction. For extraction from transgenic cells, 8 ml of cells were subcultured to 15 ml of fresh MS media and then 5-day-old cells were treated with 5 μM β-estradiol for the time shown in Figure 4-2 before extraction. Ten microgram of resulting RNA samples were subjected to on-column DNA digestion with the RNase-free DNase set (QIAGEN, www.qiagen.com/), and purified using RNeasy spin column (QIAGEN, www.qiagen.com/). Then, 500 ng (for *SOL1* expression analysis) or 1 μg (for other samples) of purified RNAs were reverse-transcribed by Superscript III (Life Technologies, www.lifetechnologies.com/) to produce cDNA.

qRT-PCR analysis

qRT-PCR analyses were carried out on Roche Lightcycler using the Lightcycler Taqman Master and Universal Probe Library (Roche Applied Science, www.roche-applied-science.com). Fifty nanogram of cDNA was used for each reaction. Primer/probe pairs used for qRT-PCR are as follows: SOL1-L1, SOL1-R1 and probe #80 for *SOL1* (L1/R1); SOL1-L2, SOL1-R2 and probe #102 for *SOL1* (L2/R2); SOL1-L3, SOL1-R3 and probe #136 for *SOL1* (L3/R3); CLE19-L, CLE19-R and probe #155 for *CLE19*; CLV3-155F, CLV3-155R and probe #155 for *CLV3*; WOX4LP, WOX4RP and probe #22 for *WOX4*; WUSLP, WUSRP and probe #33 for *WUS*;

TUA4-22F, TUA4-22R and probe #22 for *TUA4* (*tubulin α4 chain*) as a control. Sequences of these primers are shown in Table 2-1 and 2-2.

Transient gene expression in *Nicotiana benthamiana*

R. radiobacter strains GV3101::pMP90 carrying expression constructs were grown in YEB media (5 g/l beef-extract, 1 g/l yeast-extract, 5 g/l peptone, 5 g/l sucrose and 2mM $MgSO_4$, adjusted to pH 7.2 using NaOH) at 27°C with appropriate antibiotics. After centrifugation at 2600 *g* for 10 minutes, they were resuspended in infiltration buffer [10 mM MES (pH 5.7), 10 mM $MgCl_2$ and 150 mM acetosyringone]. The cultures were adjusted to OD_{600} = 1.0 and left at room temperature for 4 h before infiltration. Cultures of different constructs were mixed in appropriate ratio for coinfiltration, and then mixed with *R. radiobacter* cultures (OD_{600} = 1.0) carrying p19 silencing suppressor in a 1:1 ratio (Voinnet *et al.*, 2003). The mixed cultures were infiltrated into leaves of 3- to 4-week-old *N. benthamiana* plants for subsequent analyses.

Confocal microscopic analysis

Cultures of *R. radiobacter* strains GV3101::pMP90 (OD_{600} = 1.0) carrying the p19 silencing suppressor, estrogen-inducible SOL1-YFP and an organelle marker were mixed at a ratio of 5:4:1, and then infiltrated into *N. benthamiana* leaves for transient expression assays. The leaves were infiltrated with 10 μM β-estradiol 3 days after the first infiltration. Leaf disks from the infiltrated leaves were further incubated in 10 μM

β-estradiol at 25°C under dark conditions for 24 h. These leaf disks were observed using an LSM 710 confocal microscope (Zeiss, www.zeiss.com).

Affinity purification of SOL1-3HS

Cultures of *R. radiobacter* strains GV3101::pMP90 (OD_{600} = 1.0) carrying the p19 silencing suppressor and GV3101::pMP90 (OD_{600} =1.0) carrying estrogen-inducible *SOL1-3HS* or buffer alone (Mock) was mixed at a ratio of 1:1, and then infiltrated into *N. benthamiana* leaves for transient expression assays. Estradiol treatment was performed as above using leaf disks. Total protein was extracted from the leaf disks using twice the volume of extraction buffer (50 mM Tris-HCl, pH 8.0, 150 mM NaCl, 10% glycerol and 1% Triton X-100). Five milliliters of the lysates were centrifuged at 4°C, 20400 *g* for 20 min. Then supernatants were centrifuged again at 4°C, 20 400 *g* for 5 min. The resulting supernatants were incubated with 50 µl anti-HA affinity matrix resin (Roche Applied Science, www.roche-applied-science.com) at 4°C for 2 h with rotation. A washing step was performed using Micro Bio-Spin® chromatography columns (Bio-Rad, www.bio-rad.com). The resin was washed three times with 1 ml extraction buffer, and then four times with 500 µl extraction buffer. Prior to elution, the resin was equilibrated with 1 ml elution buffer (see below) without HA peptide. For elution, the resin was subjected three times to 100 µl elution buffer (50 mM Tris-HCl, pH 8.0, 0.05% Triton X-100 and 1 mg ml^{-1} HA peptide) at 37°C for 15 min, and the flow-through was pooled. The eluates were subjected to enzymatic assays (see below). SOL1-3HS was detected by immunoblot analysis using anti-HA 3F10 (Roche Applied

Science, www.roche-applied-science.com) as the primary antibody and goat anti-rat IgG-HRP (Santa Cruz Biotechnology, www.scbt.com) as the secondary antibody.

Enzymatic assays

All reactions were performed in a buffer containing 50 mM Tris-HCl (pH 5.0, 6.0, 7.0 or 8.0) and 0.05% Triton X-100 at 30°C in a final volume of 62.5 µl. A 5 µl aliquot of purified extract (SOL1-3HS, mock and elution buffer) and 1.25 µl of 1mM substrate [Dansyl-Phe-Ala-Arg for the fluorescence assay or CLE19+R (RVIHypTGHypNPLHNR), CLE21+K (RSIHypTGHypNPLHNK) and CLE22+R (RRVFTGHypNPLHNR) dissolved in 0.1% trifluoroacetic acid for MALDI-TOF MS] were added to the reaction. For detection of fluorescence, the reaction was stopped with 25 µl of 0.5 M HCl after incubation for the time shown in figure 3-14. Then, 500 µl of chloroform was added to the samples. Samples were mixed and then centrifuged at 200 *g* for 2 min. The fluorescence of the chloroform phase was measured at 25°C using a fluorescence spectrometer (excitation 350 nm; emission 500 nm). For MALDI-TOF MS analyses, 25 µl of anti-HA affinity matrix resin (Roche Applied Science, www.roche-applied-science.com) was added to the reaction to remove SOL1-3HS and HA peptide, and the reaction was incubated at 4°C for 1 h. After centrifugation at 4°C, 20400 *g* for 5 min, the resulting supernatant was collected and centrifuged again at 4°C, 20400 *g* for 5 min. Then, the supernatant and a-cyano-4-hydroxy-cinnamic acid were mixed at a 1:125 ratio, and masses of molecular contents of the mixture were analyzed using an Autoflex-N MALDI-TOF/TOF mass spectrometer (Bruker, www.bruker.com).

Maintenance and transformation of *Arabidopsis* cell cultures

All the cell cultures used in this study were cultivated on a rotary shaker at 23°C, 124 rpm. Composition of MS media used for all cell cultures in this study were as follows: 0.46% (w/v) Murashige and Skoog basal salts, 3% (w/v) sucrose, 0.004% (w/v) thiamine hydrochloride, 0.0004% (w/v) nicotinic acid, 0.0004% (w/v) pyridoxine hydrochloride, 0.04% (w/v) myo-inositol and 0.001% (w/v) 2,4-dichlorophenoxyacetic acid. Twelve milliliter of cell suspensions were basically subcultured to 15 ml of fresh MS medium at a one-week interval.

An *Arabidopsis* cell culture strain, Alex, which has been established from *A. thaliana* (Col-0 background) root explants, was used to produce the transgenic cell cultures. Three milliliter of 2-day-old Alex cell culture was transferred to 3 ml of fresh MS medium, to which 50 μg/ml acetosyrinegone and *R. radiobacter* carrying appropriate expression construct were added. After 2 days of co-cultivation, 6 ml of fresh MS medium and 500 μg/ml Claforan for killing bacteria were added to the culture. The culture was further cultivated for 5 days, and then transferred to 15 ml of fresh MS medium supplemented with 15 μl of 100 mg/ml Claforan. The resulting cell cultures were maintained as described above with adding 50 μg/ml Hygromycin B for selection of transformed cells. After more than 6 times of subcultures, cultured cells were used for experiments.

Microarray analysis

Eight milliliter of transgenic cells were transferred to 15 ml of fresh MS media.

Five-day-old transgenic cell cultures were treated with 5 μM β-estradiol to induce transgene expression, and collected at 0 h and 6 h. Subsequent RNA extraction and microarray analysis was performed as described in previous report (Ohashi-Ito *et al.*, 2010). The expression levels of individual genes obtained from 4 biological replicate experiments were log2-transformed for statistical analysis. Gene expression changes upon estrogen treatment were calculated for respective transgenes. WOX4-related or WUS-related genes were chosen from the comparison of gene expression changes between *ECFP* expressing cells and *WOX4-ECFP* or *WUS-ECFP* expressing cells. Student's t-test was used for selecting genes that exhibited statistically significant ($p<0.01$) expression change.

Table 2-1. Primers used in Chapter III

Primer	Sequence(5'→3')	Purpose
attB1-CLV3-F	GGGGACAAGTTTGTACAAAAAAGCAGG CTTCATGGATTCGAAGAGTTTTCTGCTAC	Amplification of *CLV3* fragment
attB2-CLV3-R	GGGGACCACTTTGTACAAGAAAGCTG GGTCTCAAGGGAGCTGAAAGTTGTTTC	
CACC+CLE19-F	CACCATGAAGATAAAGGGTTTGATGATATTG	Amplification of *CLE19* fragment
CLE19-R	TTACCTGTTGTGGAGTGGATTTGG	
attB1-CLE19-F	GGGGACAAGTTTGTACAAAAAAGCAGGC TTCATGAAGATAAAGGGTTTGATGATATTG	Amplification of *CLE19ΔR* fragment
attB2-CLE19ΔR-R	GGGGACCACTTTGTACAAGAAAGCTG GGTCTTAGTTGTGGAGTGGATTTGGACC	
pSOL1GUS-F	GGAGAGATCTGTGTTTCATTAGA GATGTTACGTCCTGTAGAAACCCC	Amplification of *GUS* fragment
GUS-R	TCATTGTTTGCCTCCCTGCTGCGG	
CACC+pSOL1-F	CACCGTTCGATCTTTTTCTTCCTTTTG	Amplification of 2370bp promoter of *SOL1*
pSOL1-R	CTCTAATGAAACACAGATCTCTCC	
CACC+SOL1CDS-F	CACCATGAGCAAGCTCAGATTCTTCC	Amplification of *SOL1* fragment without stop codon, *SOL1-3xHA-StrepII* and *SOL1-YFP*
SOL1CDS-STOP-R	TACTGTTATTGATCTTCTAGAGGATTG	Amplification of *SOL1* fragment without stop codon
StrepII-R	TTATTTTTCAAATTGAGGATGAGACC	Amplification of *SOL1-3xHA-StrepII*
EYFP-R	TTACTTGTACAGCTCGTCCATGC	Amplification of *SOL1-YFP*
SOL1-L1	GGATTTCCTTTGTGGGTCATAG	qRT-PCR: L1-R1 of *SOL1*
SOL1-R1	TCATCTCCATGTACATTCCCAAT	
SOL1-L2	GCGACTTCCCTGATCAGTTC	qRT-PCR: L2-R2 of *SOL1*
SOL1-R2	CCGACGCTGTGAATCGTAT	
SOL1-L3	TGGGCTTGTTGTGGTCAAG	qRT-PCR: L3-R3 of *SOL1*
SOL1-R3	GCAACCGATGATAGTCTGCAT	
CLE19-L	TGATATTGGCTTCTTCTCTCCTG	qRT-PCR:*CLE19*
CLE19-R	TTGAAGCTGATTCCGACTGA	
CLV3-155F	GACTTTCCAACCGCAAGATG	qRT-PCR:*CLV3*
CLV3-155R	TCATGTAGTCCTAAACCCTTCGT	
TUA4-22F	TCTTGAACATGGCATTCAGC	qRT-PCR:*TUA4*
TUA4-22R	CGGTTTCACTGAAGAAGGTGTT	

Table 2-2. Primers used in Chapter IV

Primer	Sequence(5'→3')	Purpose
cacc+WOX4CDS-f	CACCATGAAGGTTCATGAGTTTTCG	Amplification of *WOX4* fragment
WOX4CDS+stop-r	TCATCTCCCTTCAGGATGGAG	
cacc+WUSCDS-f	CACCATGGAGCCGCCACAGCATCAG	Amplification of *WUS* fragment
WUSCDS+stop-r	CTAGTTCAGACGTAGCTCAAG	
cacc+pWOX4-f	CACCTGTCCCACTTTTAGTTGTTTGG	Amplification of genomic fragment of *WOX4*
WOX4-3'-r	CACGTGAAAACCAAGAAACATTG	
pWOX4-r	TGCTATATGTTAAAACTAGCAAATG	Removing exon and intron from genomic fragment of *WOX4*
WOX4-3'-f	AGTCATGAAGGTGAGGCAGAAAATTG	
pWOX4-WOX4CDS-f	TTTTAACATATAGCAATGA AGGTTCATGAGTTTTCG	Amplification of WOX4-ECFP fragment
ECFP-WOX4 3'-r	CTCACCTTCATGACTTCAC TTGTACAGCTCGTCCATG	
WOX4LP	CATCATCGTCACTAGACATTATGAGA	qRT-PCR:*WOX4*
WOX4RP	CCTCTTGTACTCATTCTCTTCCACT	
WUSLP	AACCAAGACCATCATCTCTATCATC	qRT-PCR:*WUS*
WUSRP	TCAGTACCTGAGCTTGCATGA	
TUA4-22F	TCTTGAACATGGCATTCAGC	qRT-PCR:*TUA4*
TUA4-22R	CGGTTTCACTGAAGAAGGTGTT	

Chapter III: Analysis of processing mechanism of CLE peptides

Introduction

In *A. thaliana*, 32 *CLE* genes exist in the genome and are expressed in various tissues (Oelkers *et al.*, 2008; Jun *et al.*, 2010). These genes encode proproteins comprising approximately 100 amino acid residues, which carry an N-terminal signal peptide, the conserved 14 amino acid C-terminal CLE domain, and a less conserved variable domain between them (Cock and McCormick, 2001; Rojo *et al.*, 2002). In addition, 16 CLE proproteins possess functionally uncharacterized extension sequences that are C-terminally attached to the CLE domain (Olsen and Skriver, 2003). However, the functional roles of these C-terminal extensions are poorly understood. The biological relevance of the CLE domain was indicated by a number of experiments using chemically synthesized peptides (Fiers *et al.*, 2005; Fiers *et al.*, 2006; Ito *et al.*, 2006; Kondo *et al.*, 2006; Kinoshita *et al.*, 2007). Exogenous application of 12 amino acid synthetic peptides corresponding to the CLE domain of other CLE proteins reduced the size of the shoot apical meristem or the root length, or inhibited tracheary element differentiation (Ito *et al.*, 2006; Kondo *et al.*, 2006; Kinoshita *et al.*, 2007). Furthermore, several CLE peptides have been shown to actually function as 12/13 amino acid peptides corresponding to the CLE domain (Ito *et al.*, 2006; Kondo *et al.*, 2006; Ohyama *et al.*, 2009). These results strongly suggested that CLE peptides act as 12/13 amino acid peptides *in vivo*, and that processing steps are crucial for producing fully active CLE peptides from the CLE proproteins. However, the mechanisms underlying proteolytic processing of CLE peptides remain poorly understood.

Biochemical studies using extracts from cauliflower (*Brassica oleracea*) detected serine protease activity that cleaves the CLAVATA3 (CLV3) proprotein at the 70th arginine residue, which is located at the N-terminus of the CLE domain (Ni and Clark, 2006; Ni *et al.*, 2011). A few amino acid residues, especially the arginine located at the N-terminus of the CLE domain, are thought to be crucial for cleavage (Ni *et al.*, 2011). The cauliflower extract also exhibited carboxypeptidase activity, which may have a role in C-terminal processing (Ni *et al.*, 2011). Similarly, xylem fluid from soybean (*Glycine max*) and suspension culture fluid from barrel medic (*Medicago truncatula*) showed serine protease activity and carboxypeptidase activity that was able to produce a functional peptide from the 31 amino acid CLE36 proprotein (Djordjevic *et al.*, 2011). Despite these findings, the molecular entities responsible for these protease activities are unknown. In addition, the functional relevance of these protease activities in CLE signaling is not well understood.

Further evidence of the CLE processing machinery emerged from a suppressor mutant screening for the *CLE19* over-expression phenotype. The *suppressor of LLP1 1* (*sol1*) mutant is insensitive to root-specific *CLE19* overexpression, which normally causes root meristem consumption and a short root phenotype in the wild-type background (Casamitjana-Martínez *et al.*, 2003). *SOL1* encodes a putative Zn^{2+} carboxypeptidase with high sequence similarity to animal carboxypeptidase D (CPD) and carboxypeptidase E (CPE) (Casamitjana-Martínez *et al.*, 2003). In animals, these carboxypeptidases are known to play a role in processing of peptide hormones such as insulin (Docherty and Hutton, 1983; Varlamov *et al.*, 1997; Dong *et al.*, 1999; Davidson,

2004). In addition, biochemical analyses demonstrated that both CPD and CPE are capable of cleaving C-terminal arginine and lysine from polypeptides *in vitro* (Fricker and Snyder, 1983; Greene *et al.*, 1992; Sidyelyeva and Fricker, 2002). The strong suppressor effect of the *sol1* mutation on the *CLE19* over-expressing phenotype suggests the importance of SOL1 in proteolytic modification of the CLE19 proprotein, presumably by targeting arginine residues, to produce the active CLE19 peptide (Casamitjana-Martínez *et al.*, 2003). Thus, functional dissection of SOL1 is required to decipher its role in CLE19 signaling, and this should further advance our understanding of the complex regulation of CLE peptide signaling.

In this study, I performed a series of detailed analyses of SOL1 to unravel the processing machinery of CLE peptides. I demonstrate that two *SOL1* T-DNA insertion lines are not defective in CLV3 and CLE19 signal transduction pathways *per se*. I further show that SOL1-dependent cleavage of the C-terminal arginine is critical for CLE19 activity *in planta*, whereas SOL1 is not involved in generating active CLV3. Additionally, the results of the SOL1 localization analysis imply that C-terminal processing of CLE19 by SOL1 is likely to occur in endosomes. My biochemical analyses revealed that SOL1 cleaves not only the C-terminal arginine but also lysine, implying a role in processing of CLE peptides other than CLE19. These findings provide insight into our understanding of the CLE peptide maturation process, which may act as an additional regulatory step for CLE signaling.

Results

The SOL1 expression pattern indicates its involvement in many developmental processes

To determine the function of SOL1 and its potential target CLEs, I first examined the expression pattern of *SOL1*. The 2370 bp *SOL1* upstream sequence fused to the β-glucuronidase (GUS) reporter gene was transformed into Columbia-0 (Col-0) plants (Figure 3-1a). The GUS activity of the resulting transgenic T_2 plants was analyzed. Microscopic observation detected GUS activity in columella cells, the lateral root cap, stipules and young true leaves, with stronger expression in the basal regions (Figure 3-1b–d). Although weak GUS activity was also detected in cotyledons and the basal region of developed leaves, no activity was detected in the lateral root primordia and the shoot apical meristem (Figure 3-1e–h). Thus, *SOL1* is expressed in various tissues, and may therefore contribute to multiple functions in *Arabidopsis*. This ubiquitous localization may allow SOL1 to act as a generic maturation enzyme for proproteins of CLE family members, which are also expressed in various tissues (Jun *et al.*, 2010).

The *sol1* mutation does not alter responsiveness to the CLV3 and CLE19 peptides

To further explore the function of SOL1, I isolated two *SOL1* T-DNA insertion lines (in the Col-0 background) from the SALK lines SALK_013659c and SALK_015449c, designated *sol1-101* and *sol1-102*, respectively. These lines contain T-DNA insertions in the 8th and the 14th exons, respectively (Figure 3-2 and 3-3a). Transcripts for *sol1-101* and *sol1-102* were examined by quantitative qRT-PCR using three primer

pairs: L1/R1 (located outside the T-DNA insertion site), L2/R2 (flanking the T-DNA insertion site of the *sol1-101* mutant) and L3/R3 (flanking the T-DNA insertion site of the *sol1-102* mutant) (Figure 3-3a). The L1/R1 primer pair amplified as much transcript for *sol1-101* and *sol1-102* as for wild-type. No transcript was detected in the *sol1* mutants using the primer pairs containing the T-DNA insertion sites for the respective mutant genes (L2/R2 for *sol1-101* and L3/R3 for *sol1-102*), although the other primer pairs detected as much transcripts as wild-type even in the *sol1* mutants (Figure 3-3b). This result indicates that the *sol1-101* and *sol1-102* genes are not correctly transcribed, and may produce longer transcripts containing the T-DNA sequence or two transcripts split by T-DNA. Therefore, both alleles were considered to produce incomplete SOL1 proteins. For further characterization, I mainly focused on *sol1-101* as the mutated protein produced in the *sol1-101* mutant is thought to lack both the conserved catalytic residues and the transmembrane domain while the *sol1-102* protein lacks only the transmembrane domain, which may express its residual activity (Figure 3-2).

I examined the *sol1* mutant in a root growth inhibition assay using chemically synthesized 12 amino acid forms of CLE19 (RVIHypTGHypNPLHN, where Hyp is hydroxyproline) and CLV3 (MCLV3, RTVHypSGHypDPLHH). CLE19 is the most likely candidate for a substrate of SOL1 as suggested by a previous report, and CLV3 is the best-studied CLE member (Casamitjana-Martínez *et al.*, 2003). Both MCLV3 and CLE19 treatments reduced root growth in all plants tested, and no significant differences were observed among *sol1-101*, *sol1-102* and wild-type (Figures 3-4, 3-5 and 3-6). This result indicates that the *sol1* mutants are not defective in the endogenous

CLV3 and CLE19 signaling pathways, consistent with the hypothesis that SOL1 is involved in the maturation of CLE peptides.

The *sol1* mutations suppress the *CLE19* over-expression phenotype, but not the *CLV3* over-expression effect

My root inhibition assay using the newly isolated *sol1* mutants and the CLE peptides revealed that SOL1 is not required for perception of CLE19 or CLV3, although the original *sol1* mutation was shown to suppress the phenotype caused by root-specific over-expression of *Brassica napus CLE19* (Casamitjana-Martínez *et al.*, 2003). Therefore, I investigated the impact of the *sol1* mutation on the *CLE19* and *CLV3* over-expression phenotypes. For this purpose, I generated stable transgenic wild-type and *sol1-101* plants expressing either full-length *CLV3* or *CLE19* under the control of an estrogen-inducible promoter. My qRT-PCR analyses revealed that β-estradiol treatment induces the expression of respective transgenes to a similar extent in Col-0 and *sol1-101* background plants (Figures 3-7 and 3-8). The conditional expression of *CLE19* by β-estradiol reduced the root length of plants in the wild-type background (Figures 3-9a and 3-10), but not in the *sol1-101* background (Figures 3-9b and 3-11), consistent with the findings of the previous study (Casamitjana-Martínez *et al.*, 2003). However, the inhibition of root growth by estrogen-induced *CLV3* expression was not affected by the *sol1-101* mutation (Figures 3-9c,d, 3-12 and 3-13). Thus, my data are consistent with the results of a previous study suggesting that SOL1 is involved in CLE19 maturation, but not in CLE19 perception (Casamitjana-Martínez *et al.*, 2003).

Furthermore, this result strongly suggests that SOL1 is preferentially involved in the maturation process of CLE19, but not CLV3.

In support of this idea, the *sol1* mutants did not show an enlargement of the shoot apical meristem, a phenotype that is a hallmark of CLV3-related mutants (Clark *et al.*, 1993; Clark *et al.*, 1995; Kayes and Clark, 1998; Müller *et al.*, 2008; Kinoshita *et al.*, 2010). To uncouple SOL1 activity from the CLV3 pathway genetically, I performed phenotypic analysis of crosses between the *sol1* mutant and the CLV3-related mutants *clavata1-101* (*clv1-101*), *clavata2-101* (*clv2-101*), *receptor-like protein kinase 2-2* (*rpk2-2*) and *clv3-8* (Diévart *et al.*, 2003; Kinoshita *et al.*, 2010). I counted the number of carpels in the ten basal flowers of the inflorescence stem of Col-0, *sol1-101*, *sol1-102*, *clv1-101*, *clv1-101 sol1-101*, *clv2-101*, *clv2-101 sol1-101*, *rpk2-2*, *rpk2-2 sol1-101*, *clv3-8* and *clv3-8 sol1-101*. I found that the presence of the *sol1* mutation did not significantly increase the carpel number of any double mutants compared to the respective single mutants (Table 3-1). Together with the data for estrogen-induced *CLV3* expression in *sol1-101*, I conclude that SOL1 is not required for CLV3 maturation.

SOL1 possesses *in vitro* carboxypeptidase activity against the C-terminal arginine and lysine

The ability of CPD and CPE, animal homologs of SOL1, to cleave the C-terminal arginine or lysine residues from polypeptides prompted me to speculate that SOL1 may be involved in C-terminal maturation of CLE proproteins (Fricker and Snyder, 1983;

Greene *et al.*, 1992; Sidyelyeva and Fricker, 2002). To characterize the *in vitro* carboxypeptidase activity of SOL1, SOL1 C-terminally fused to a triple hemagglutinin (HA)/single StrepII tag (*SOL1-3HS*) was transiently expressed in *Nicotiana benthamiana* leaves and then affinity-purified (Figure 3-14a). Purified protein was detected as two major bands, which may reflect the presence or absence of the signal peptide (Figure 3-14a). To investigate carboxypeptidase activity of the purified SOL1-3HS, Dansyl-Phe-Ala-Arg, a well-established artificial fluorescent substrate of CPD and CPE, was used (Fricker and Snyder, 1983; Greene *et al.*, 1992; Sidyelyeva and Fricker, 2002). The reaction with the purified SOL1-3HS significantly increased the fluorescence of Dansyl-Phe-Ala, the cleaved product, compared to the mock reaction and buffer alone (Figure 3-14b). Lower pH conditions significantly reduced the cleavage activity, suggesting that SOL1 functions in neutral pH conditions *in vivo* (Figure 3-14c). These results show that SOL1 possesses carboxypeptidase activity to remove the arginine residue from Dansyl-Phe-Ala-Arg, indicating that an additional arginine at the C-terminus of the CLE domain of CLE19 may be targeted and removed by SOL1. Therefore, I directly examined SOL1 activity using a synthetic CLE19 peptide derivative containing the C-terminal arginine after the CLE domain (CLE19+R). After incubating CLE19+R with the purified fractions, MALDI-TOF MS analysis was performed in corporation of Dr. Masayuki Fujiwara (NAIST, Japan) and Dr. Yoichiro Fukao (NAIST, Japan) and detected the 12 amino acid CLE19 peptide processed from CLE19+R only in the reaction containing purified SOL1-3HS (Figure 3-15a,b). This result strengthens my hypothesis. I also performed the same experiment using synthetic

CLE21+K and CLE22+R peptides. SOL1 cleaved the C-terminal arginine or lysine of CLE21+K and CLE22+R (Figures 3-16 and 3-17). Collectively, these results imply that SOL1 cleaves both lysine and arginine at the C-terminus, which suggests the involvement of SOL1 in processing of other CLE proproteins that harbor R or K at their C-terminus.

The suppressor effect of *sol1-101* depends on the C-terminal arginine of the CLE19 proprotein

Having established that the recombinant SOL1-3HS produced in *N. benthamiana* possesses carboxypeptidase activity that removes the C-terminal arginine residue from the synthetic 13 amino acid CLE19+R peptide, I examined whether SOL1 acts against the CLE19 proprotein in plant tissues. The *sol1* mutants were insensitive to estrogen-induced *CLE19* expression, presumably due to their inability to process the CLE19 proprotein in the absence of SOL1 (Figure 3-9b). If this is indeed the case, then the *sol1* mutants should be sensitive to estrogen-induced expression of *CLE19* lacking C-terminal arginine (designated *CLE19*Δ*R*; Figure 3-18a). To test this hypothesis, I transformed wild-type and *sol1-101* plants with *CLE19*Δ*R* under the control of the estrogen-inducible promoter. β-estradiol treatment clearly inhibited root growth of the transgenic Col-0 plants expressing *CLE19*Δ*R*, as it did for Col-0 plants over-expressing full-length *CLE19* (Figures 3-18b and 3-19). The estrogen-induced expression of *CLE19*Δ*R* also reduced the root length of the transgenic *sol1-101* plants (Figures 3-18c and 3-20). This result is in contrast to the insensitivity of the *sol1-101* mutant to

estrogen-induced expression of the full-length *CLE19* (Figure 3-9b). This result strongly suggests that SOL1 processes the C-terminal arginine of the CLE19 proprotein. It also suggests that this SOL1-mediated C-terminal processing is crucial for production of active CLE19 peptide *in planta*.

SOL1 is localized specifically to endosomes

CLE proproteins undergo proteolytic maturation processes that produce functional CLE peptides, which are subsequently secreted into apoplastic spaces, where they function (Rojo *et al.*, 2002). In this study, I showed that the C-terminal maturation of CLE19 is mediated by SOL1, a putative membrane-bound carboxypeptidase (Casamitjana-Martínez *et al.*, 2003). However, it remains to be determined in which compartment of the secretory pathway CLE proproteins are processed into mature functional peptides. To address this question, I analyzed the subcellular localization of SOL1, a CLE-processing enzyme. For this purpose, I transiently expressed *SOL1-YFP* under the control of an estrogen-inducible promoter in the leaves of *N. benthamiana*, together with the known organelle markers *35S:SP-GFP-HDEL*, an endoplasmic reticulum (ER) marker (Mitsuhashi *et al.*, 2000), *35S:ST-mRFP*, a trans-Golgi marker (Boevink *et al.*, 1998), *35S:mRFP-SYP61*, a trans-Golgi network marker (Sanderfoot *et al.*, 2001; Uemura *et al.*, 2004) or *35S:TagRFP-ARA6*, an endosomal marker (Ueda *et al.*, 2001). Confocal microscopic observation revealed that SOL1-YFP localized to dot-like organelles inside the estrogen-treated cells, suggesting that SOL1 localizes to the endomembrane system other than the plasma membrane (Figure 3-21). The

co-expression study showed that SOL1-YFP did not co-localize with SP-GFP-HDEL or ST-mRFP, but occasionally localized with mRFP-SYP61 and more frequently with TagRFP-ARA6, indicating that SOL1-YFP preferentially localizes to the endosomes (Figure 3-21a-d). I therefore used TagRFP-ARA7 as another endosomal marker (Sohn *et al.*, 2003; Kotzer *et al.*, 2004), and found that it showed almost fully overlapping localization with SOL1-YFP (Figure 3-21e). These data indicate that SOL1 is mainly localized to endosomes, and, occasionally, to the trans-Golgi network, suggesting that C-terminal processing of the CLE19 proprotein occurs in endosomes.

Discussion

SOL1 has been implicated as a peptidase involved in processing of the CLE19 proprotein (Casamitjana-Martínez *et al.*, 2003). My biochemical analysis showed that SOL1 is capable of removing the C-terminal arginine or lysine from CLE proproteins *in vitro*. I suggest that SOL1-mediated removal of the arginine is essential for CLE19 activity *in planta*. These results suggest a critical role for SOL1 in CLE19-mediated signaling *in planta*.

SOL1 generates active CLE19 through post-translational processing

Peptide hormones regulate various aspects of animal and plant development. In many cases, peptide hormones are first translated as inactive precursor polypeptides, and become active through post-translational processing (Fricker, 1988). It is considered that such processing, in addition to transcriptional regulation, enables organisms to release peptide hormone activities at accurate times during development (Muller *et al.*, 1999; Westphal *et al.*, 1999). To understand the processing of CLE peptides, which are the best known signaling peptides acting in plant development, I analyzed the processing of CLE19. I showed that SOL1-dependent processing of the CLE19 proprotein is essential for CLE19 activity. My biochemical experiments revealed that SOL1 exhibits *in vitro* processing activity with respect to the C-terminal arginine of the CLE19 polypeptide. In addition, conditional over-expression of *CLE19* and *CLE19*Δ*R* also indicated the importance of SOL1 activity in removal of the C-terminal arginine of

the CLE19 proprotein *in vivo*. Addition of the C-terminal arginine to TRACHEARY ELEMENT DIFFERENTIATION INHIBITORY FACTOR (TDIF), another well-studied CLE peptide, reduces its activity to one-seventh (Ito *et al.*, 2006). Thus, these results suggest that the C-terminal arginine processing performed by SOL1 or SOL1-like enzymes is a critical step for generating active CLE peptide.

Biochemical activity may be used for identifying other SOL1-targeted CLE peptides

Several CLE proproteins harbor a C-terminal arginine, in addition to CLE19 (Figure 3-22). It has been reported that CPD and CPE, the animal SOL1 homologs, cleave not only C-terminal arginine residues but also C-terminal lysine residues of their substrates (Fricker and Snyder, 1983; Greene *et al.*, 1992; Sidyelyeva and Fricker, 2002). Hence, the same activity may be predicted for SOL1, and SOL1 showed *in vitro* enzymatic activity against the C-terminal arginine and lysine of Dansyl-Phe-Ala-Arg, CLE19+R, CLE21+K and CLE22+R peptides. Amongst *Arabidopsis* CLE proproteins, CLE14, CLE20, CLE21, CLE22 and CLE42 possess a C-terminal arginine or lysine residue directly after their CLE domains, and are designated RK type, suggesting that these CLE proproteins are good candidates for SOL1 *in planta* substrates (Olsen and Skriver, 2003). Simultaneous overexpression of *SOL1* and *CLE19* in *sol1* mutants successfully demonstrated SOL1 activity against CLE19 proprotein. Therefore, similar methods may be used to identify additional CLE substrates of SOL1. In addition to this RK type of

CLE peptide, there is a group of CLE peptides, including CLE25, CLE26, CLE40, CLE45 and CLE46, that contains a CLE domain-Arg/Lys-X motif (RK embedded type, where X represents any polypeptide). It is reasonable to assume that primary removal of the C-terminal polypeptides (X) from these CLEs by peptidases reveals the arginine or lysine residue flanking the CLE domain, which may then be processed by SOL1. Thus, these CLEs are also possible substrates of SOL1 (Olsen and Skriver, 2003). For example, *CLE40*, which is expressed in the columella cells of root tips, as *SOL1* is, possesses a lysine residue directly after the CLE domain, and the lysine is followed by an additional six amino acid stretch (Olsen and Skriver, 2003; Stahl *et al.*, 2009). Additionally, *CLE21*, *CLE25* and *CLE26* are expressed in the shoot apices, young leaves and tips of young leaves, respectively (Jun *et al.*, 2010). These expression patterns also resemble those of *SOL1*, further supporting my hypothesis. Thus, the presence of the buried arginine or lysine residue in the RK embedded type motif implies that a two-step C-terminal processing mechanism is involved in maturation of these CLEs. Such a mechanism would strongly ensure precise regulation of these CLE activities. Further analyses of SOL1, focusing on CLE peptides containing these RK embedded type motifs, are required to provide further insights into as yet unknown functions of CLE peptides.

Localization analysis links C-terminal processing of CLE19 and ARA6 endosomes

CLE peptides are secretory signaling molecules. Processing of CLE proproteins is thought to occur in extracellular spaces after secretion (Ni and Clark, 2006; Djordjevic

et al., 2011; Ni *et al.*, 2011). Recent research suggests that secreted serine proteases may be involved in N-terminal processing of CLE peptides (Djordjevic *et al.*, 2011; Ni *et al.*, 2011). However, my findings provide another possibility for the CLE peptide maturation pathway. As SOL1 possesses a signal peptide and transmembrane domain, I predicted that SOL1 localizes to the endomembrane system. Subcellular localization analyses indicated that SOL1 localizes mainly to ARA7-positive endosomes, and, to a lesser extent, ARA6-positive endosomes. In agreement with this, animal homologs of SOL1 have been reported to localize to the trans-Golgi network and secretion vesicles (Docherty and Hutton, 1983; Hook and Loh, 1984; Varlamov *et al.*, 1999). The protein structure of SOL1 predicted by SignalP (http://www.cbs.dtu.dk/services/SignalP/) indicates that the enzymatically active part of SOL1 locates towards the inside of the vesicle, suggesting its role in processing of vesicle content, consistent with a previous report on CPD (Varlamov and Fricker, 1998). ARA7 is known to function in vacuolar transport from endosomes (Sohn *et al.*, 2003; Kotzer *et al.*, 2004). ARA6 is suggested to mediate vesicle transport from ARA7-positive endosomes to the plasma membrane (Ebine *et al.*, 2011). Although SOL1 highly colocalized with ARA7, CLE19, a substrate of SOL1, is considered to be secreted into the extracellular space (Rojo *et al.*, 2002). I demonstrated that SOL1 loses its activity under low pH, suggesting that SOL1-mediated C-terminal maturation of CLE19 occurs in the endosomes, but not in the acidic vacuole, before branching of the ARA6-mediated secretory pathway and ARA7-mediated vacuolar transport pathway. Thus, I propose a model for CLE19 secretion. First, the CLE19 proprotein is C-terminally processed by SOL1 in ARA7-positive endosomes.

Second, the processed precursor is secreted through the ARA6-mediated secretion pathway to the apoplast, in which N-terminal processing is performed by serine proteases. After CLE19 processing in ARA6- and ARA7-positive endosomes, SOL1 may be carried via the ARA7 pathway to the vacuoles for degradation. The plant-unique ARA6-dependent secretory pathway is proposed to participate in environmental responses, such as salinity resistance (Ebine*, et al.*, 2011). In this context, CLE19 may contribute to achieving an orchestrated developmental plasticity in response to various environmental conditions. The post-translational regulation of CLE19 through SOL1 activity may add another level of regulation in response to environmental cues. Detailed studies of CLE19 activity and its SOL1-dependent regulation should provide insights into the role of the CLE19 peptide as a signaling molecule.

Post-translational control provides another layer of CLE activity regulation

The *A. thaliana* genome encodes 32 *CLE* genes corresponding to at least 27 CLE peptides (Oelkers *et al.*, 2008). A chemical genetics approach using 26 synthetic CLE peptides functionally categorized these peptides into four groups, indicating highly redundant activity within groups (Ito *et al.*, 2006; Kinoshita *et al.*, 2007; Hirakawa *et al.*, 2011; Kondo *et al.*, 2011). In contrast, a comprehensive analysis of their promoter activities revealed distinct and characteristic expression patterns (Jun *et al.*, 2010). These results suggest that plant development is fine-tuned through complex and precise transcriptional regulation of various *CLE* genes. Here, I raised the possibility that peptidase-mediated post-translational processing may be another important layer in the

control of CLE activities, at least in the case of CLE19. My study also highlights involvement of the plant-unique ARA6-mediated secretory pathway in the CLE19 maturation process (Ebine *et al.*, 2011). Thus, further studies of the CLE19 maturation process are required to determine the biological relevance of the plant-unique secretory pathway in CLE peptide production. Furthermore, identification of other peptidase(s) required for the N- and C-terminal processing of CLE proproteins is the next challenge in achieving a comprehensive understanding of CLE-mediated plant morphogenesis.

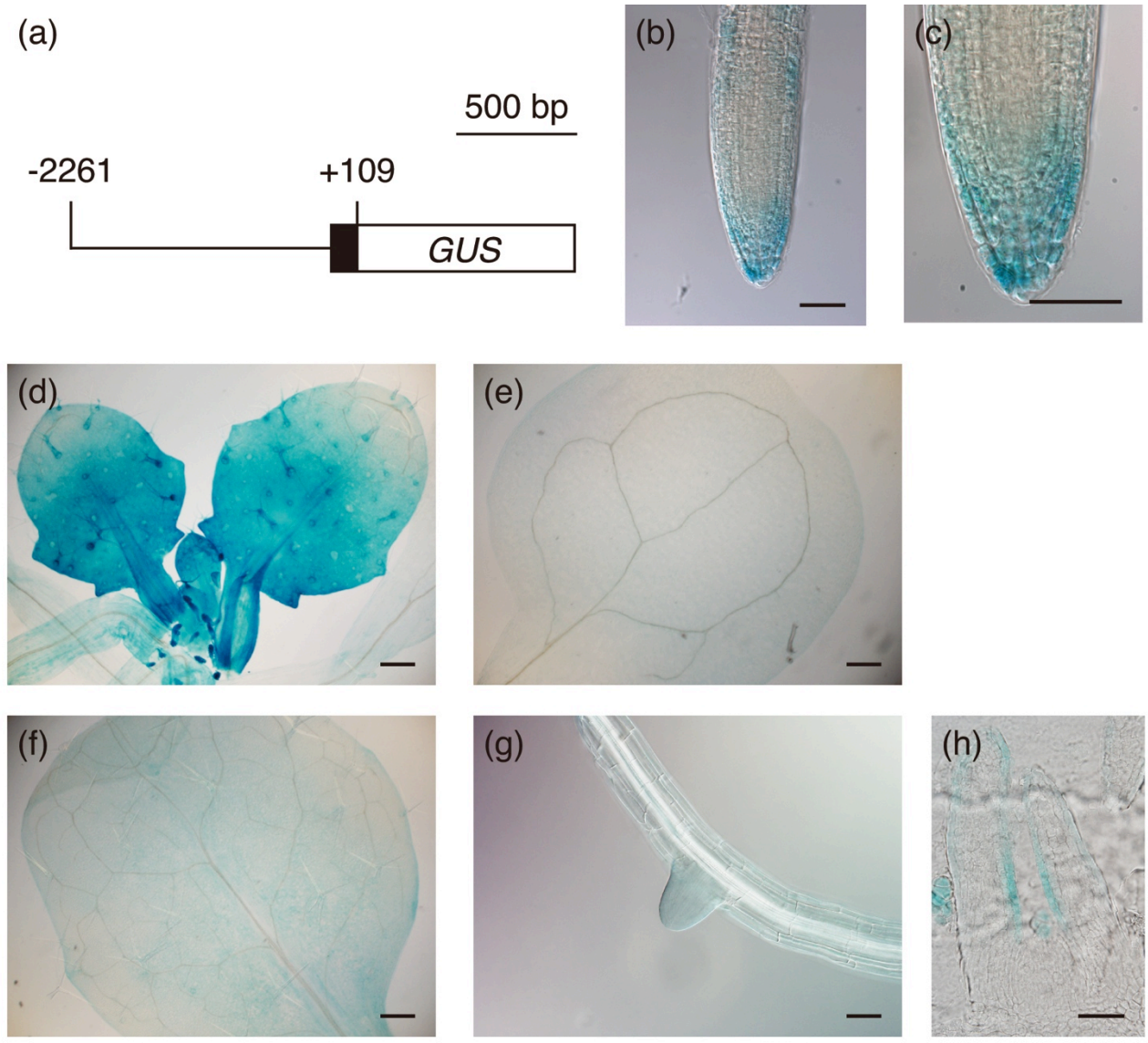

Figure 3-1. Tissue-specific expression pattern of *SOL1*
(a) Structure of the *SOL1*$_{pro}$*:GUS* construct. The 2370 bp upstream sequence of *SOL1* was fused to the *β-glucuronidase* (*GUS*) reporter gene. Black box indicates the 5' UTR of *SOL1*.
(b)-(h) Transgenic T_2 plants carrying the *SOL1*$_{pro}$*:GUS* reporter gene were stained for GUS activity.
(b) Primary root tip. (c) High magnification image of primary root tip. (d) Young leaves. (e) Cotyledon. (f) Developed true leaf. (g) Lateral root primordium. (h) 10 μm section of the SAM.
Scale bars = 200 μm in (d), (e) and (f) and 50 μm in the other panels.

Figure 3-2. The amino-acid sequence and catalytic residues of SOL1 protein Arrowhead indicates the putative signal peptide cleavage site and the putative transmembrane domain is underlined. For prediction of the cleavage site, I used SignalP 3.0 Server (http://www.cbs.dtu.dk/services/SignalP/). For prediction of the transmembrane domain, I used TMHMM Server v. 2.0 (http://www.cbs.dtu.dk/services/TMHMM/). Other carboxypeptidase conserved residues are exhibited as previous study. The H, E and H residues responsible for Zn^{2+} binding are depicted with an asterisk. The R and Y residues required for substrate binding are boxed with a square. The catalytic E residue is circled. T-DNA insertion sites of the *sol1-101* and *sol1-102* mutants are also indicated with arrows.

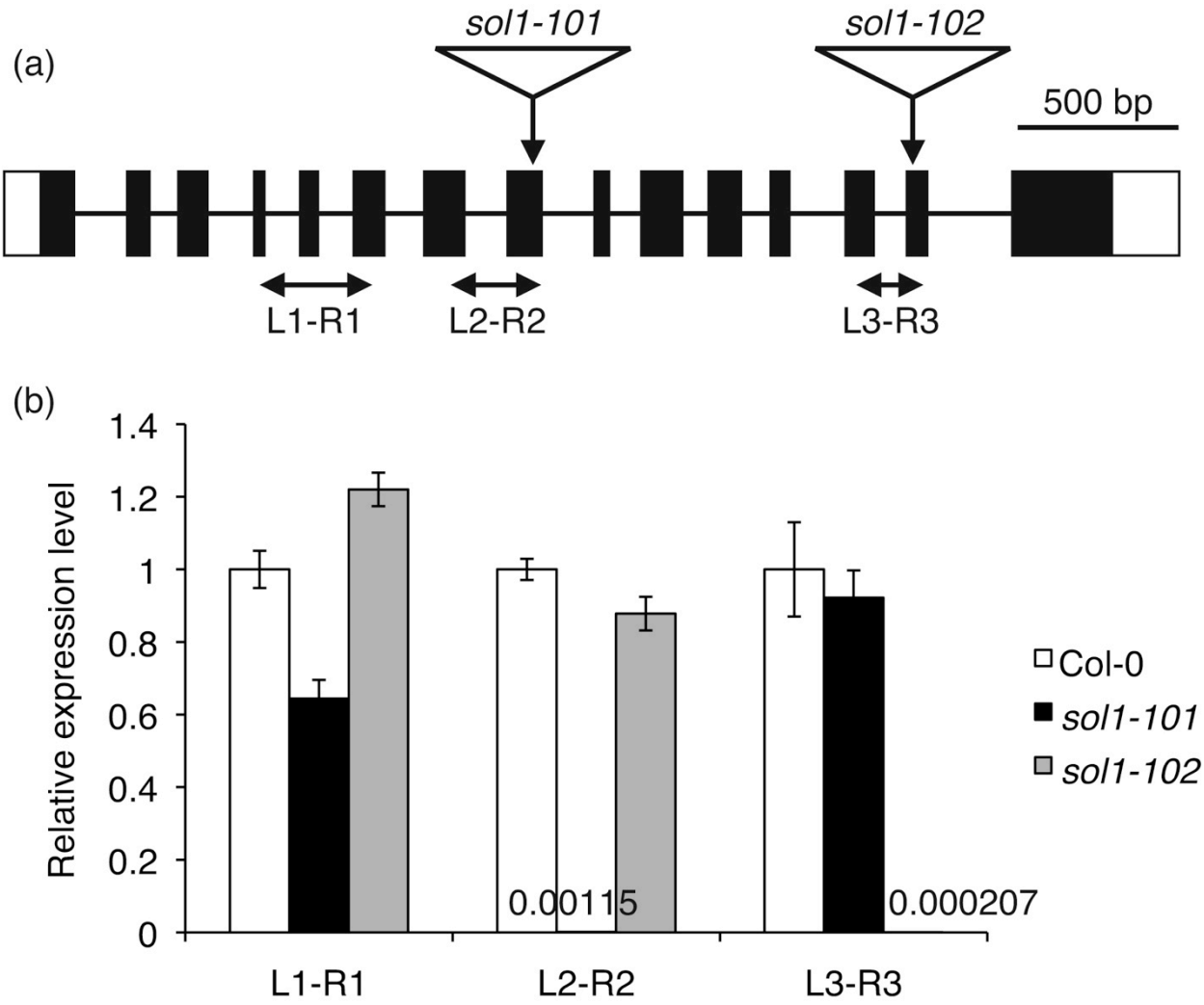

Figure 3-3. Characterization of the *sol1* mutants
(a) Gene structure of *SOL1*. The white boxes indicate 5' - and 3' - untranslated regions. The black boxes indicate exons. The black bars indicate introns. T-DNA insertion sites and the amplification sites of the primer sets, L1-R1, L2-R2 and L3-R3 are shown.
(b) qRT-PCR analysis of expression levels of *SOL1* using total RNAs from whole seedlings of Col-0, *sol1-101* and *sol1-102* grown on 1/2 MS agar plates for 16 days (n=4~5; mean ± SEM).

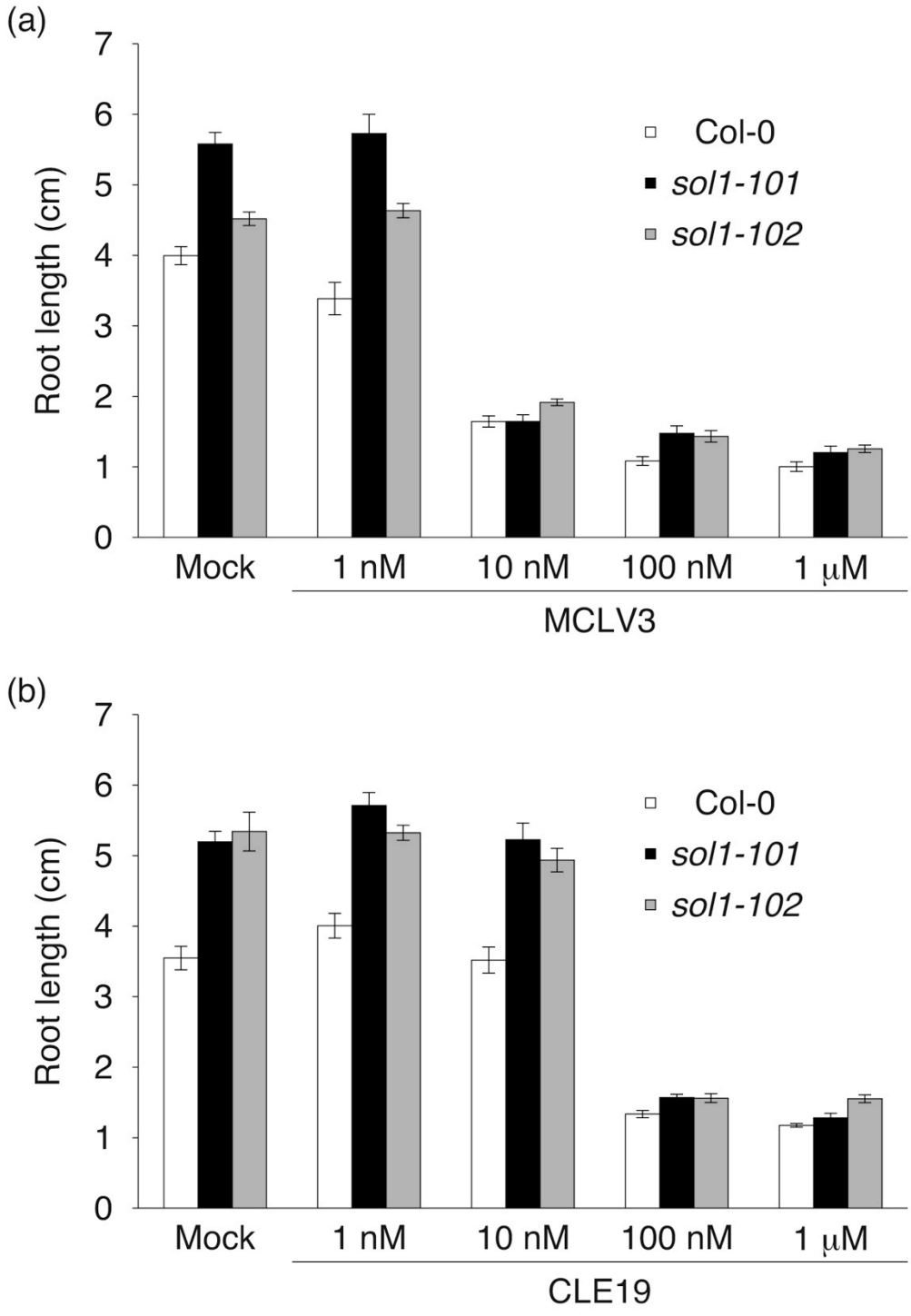

Figure 3-4. Effects of the MCLV3 and CLE19 peptides on root growth of the *sol1* mutants
(a) Primary root length of seedlings treated with various concentrations of MCLV3 (n=9~11; mean ± SEM).
(b) Primary root length of seedlings treated with various concentrations of CLE19 (n=9~11; mean ± SEM).

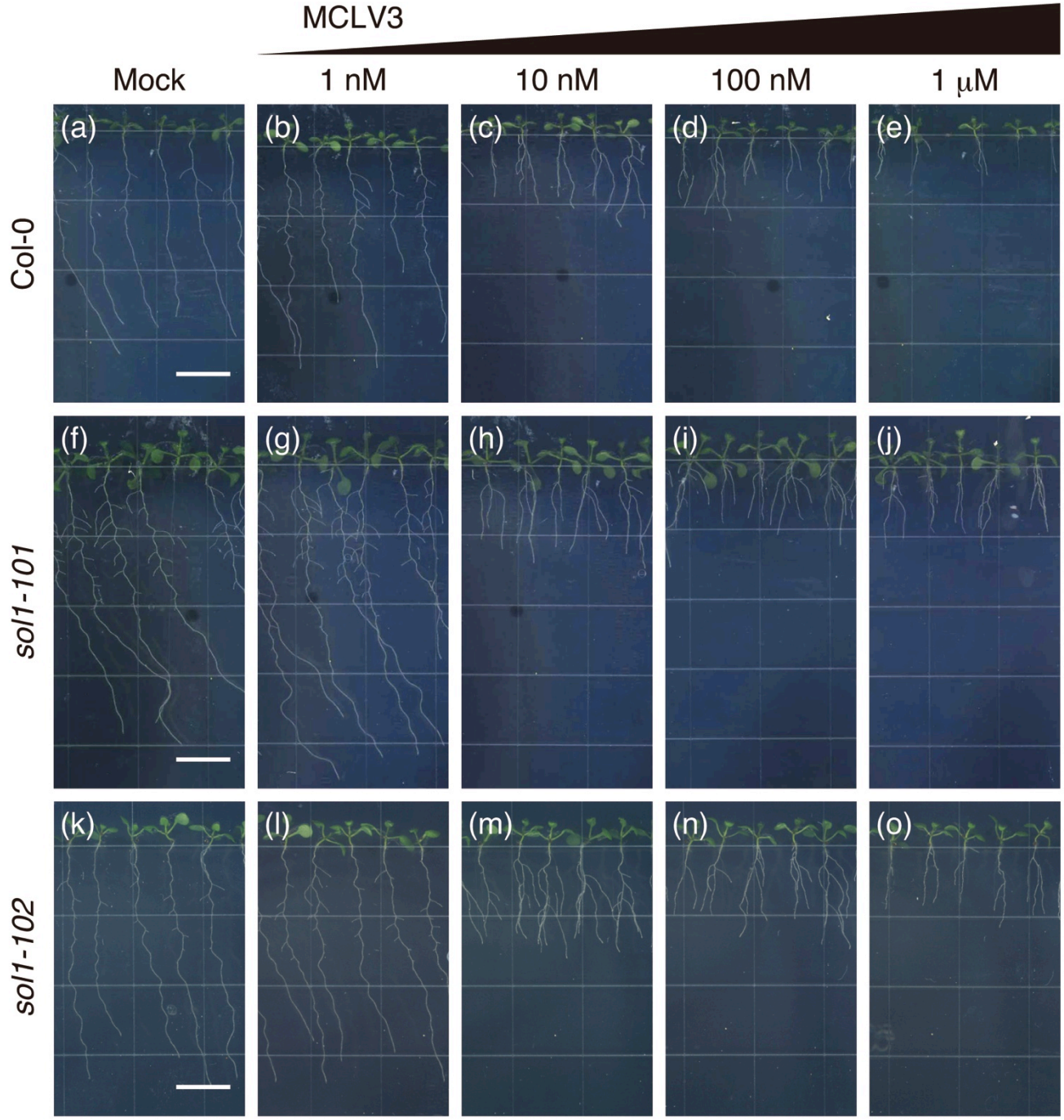

Figure 3-5. Effects of MCLV3 treatment on Col-0 and *sol1* mutants
Col-0 (a-e), *sol1-101* (f-j) and *sol1-102* (k-o) plants were grown on 1/2 MS agar plates containing various concentrations of the MCLV3 peptide for 9 days.
(a), (f) and (k) Mock treatment. (b), (g) and (l) 1 nM MCLV3 treatment.
(c), (h) and (m) 10 nM MCLV3 treatment. (d), (i) and (n) 100 nM MCLV3 treatment.
(e), (j) and (o) 1 μM MCLV3 treatment.
Scale bars = 1 cm.

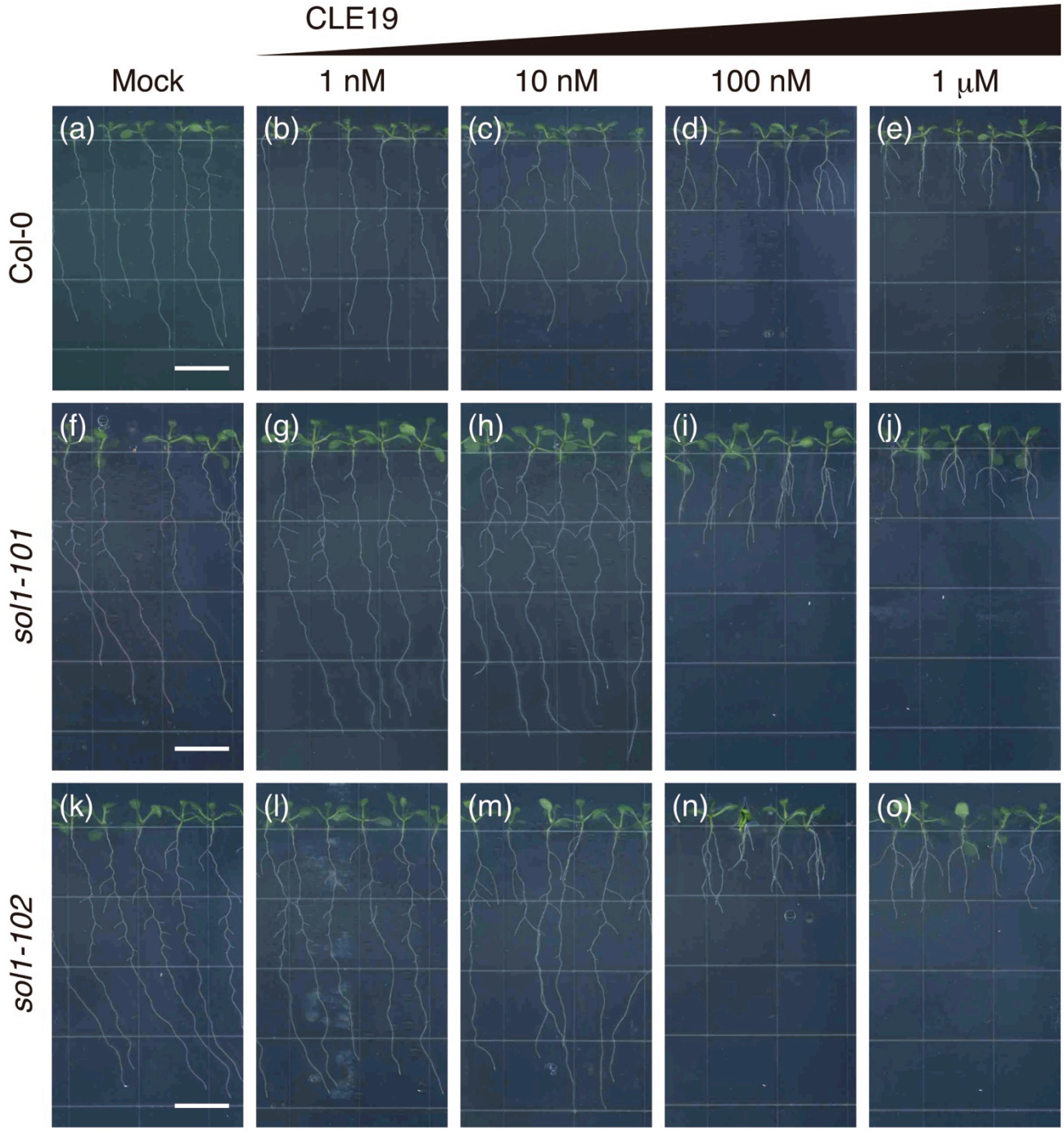

Figure 3-6. Effects of CLE19 treatment on Col-0 and *sol1* mutants
Col-0 (a-e), *sol1-101* (f-j) and *sol1-102* (k-o) plants were grown on 1/2 MS agar plates containing various concentrations of the synthetic CLE19 peptide for 9 days. (a), (f) and (k) Mock treatment. (b), (g) and (l) 1 nM CLE19 treatment. (c), (h) and (m) 10 nM CLE19 treatment. (d), (i) and (n) 100 nM CLE19 treatment. (e), (j) and (o) 1 μM CLE19 treatment.
Scale bars = 1 cm.

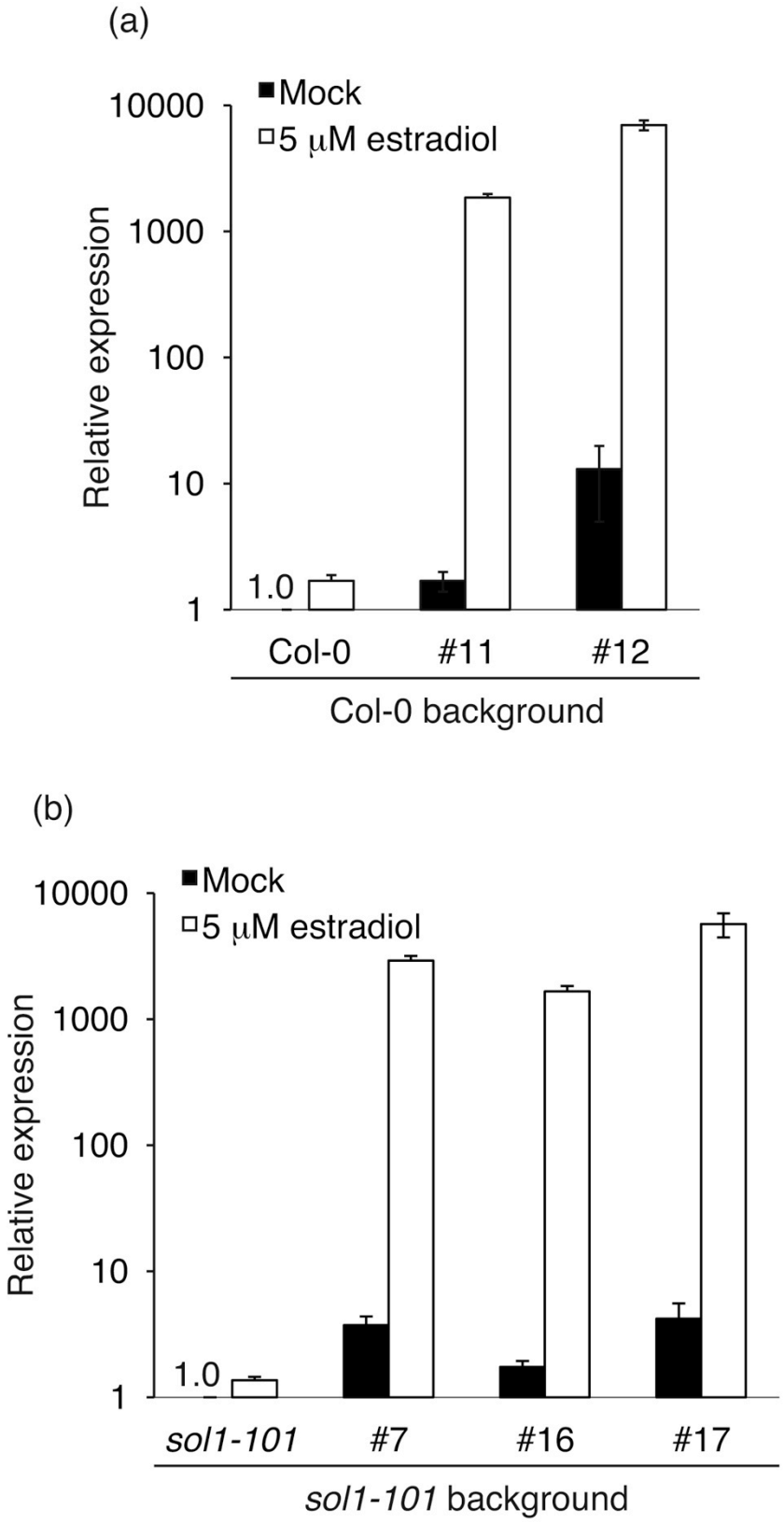

Figure 3-7. Estrogen-induced expression of *CLE19*
qRT-PCR analysis of *CLE19* expression using total RNA from whole seedlings . Plants were grown for 9days in liquid 1/2 MS media and then treated with 10 μM β-estradiol for 24 h.
(a) Col-0 background plants (n=3; mean ± SEM). (b) *sol1-101* background plants (n=3; mean ± SEM).

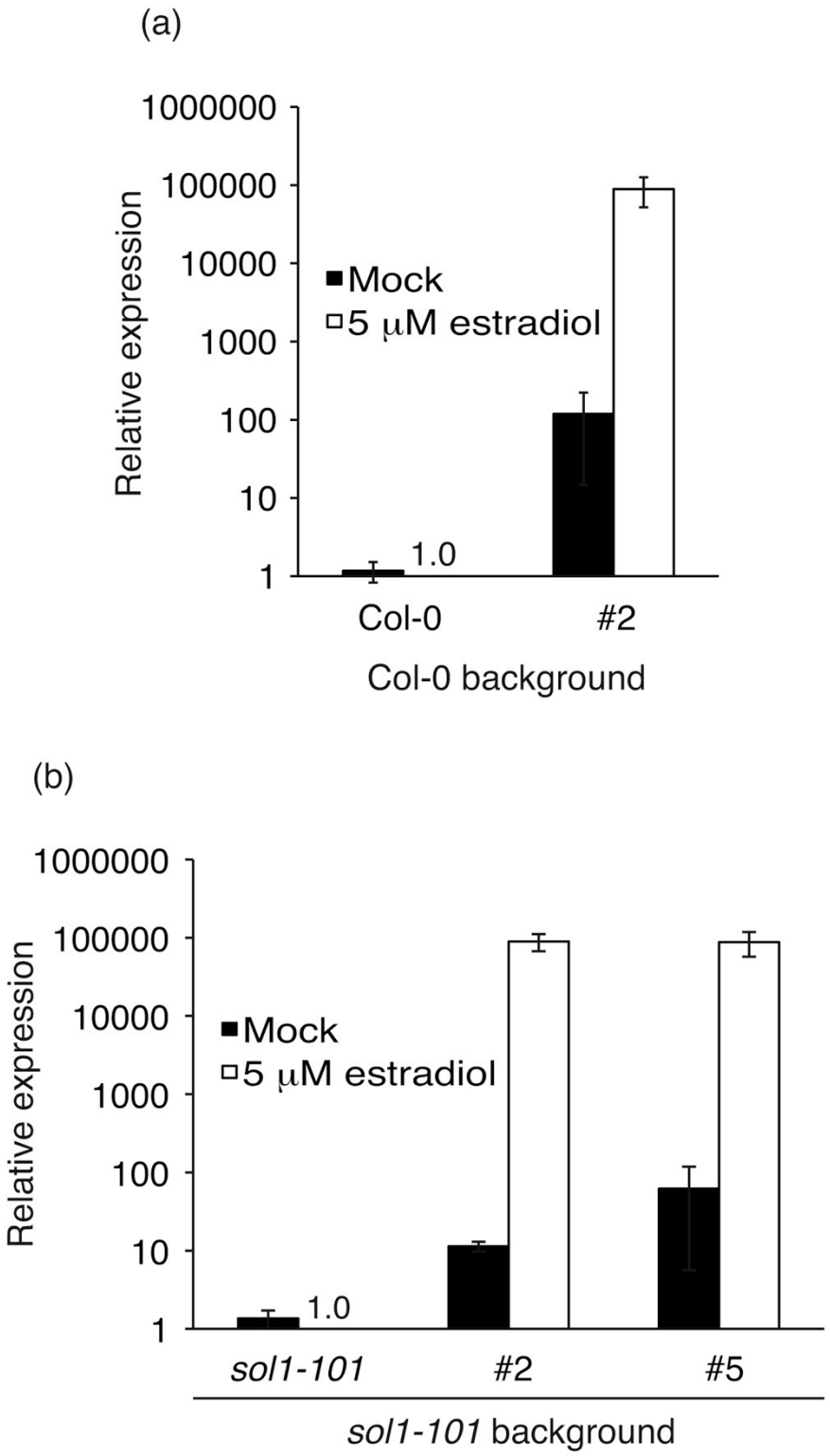

Figure 3-8. Estrogen-induced expression of *CLV3*
qRT-PCR analysis of *CLV3* expression using total RNA from whole seedlings . Plants were grown for 9days in liquid 1/2 MS media and then treated with 10 μM β-estradiol for 24 h.
(a) Col-0 background plants (n=3; mean ± SEM). (b) *sol1-101* background plants (n=3; mean ± SEM).

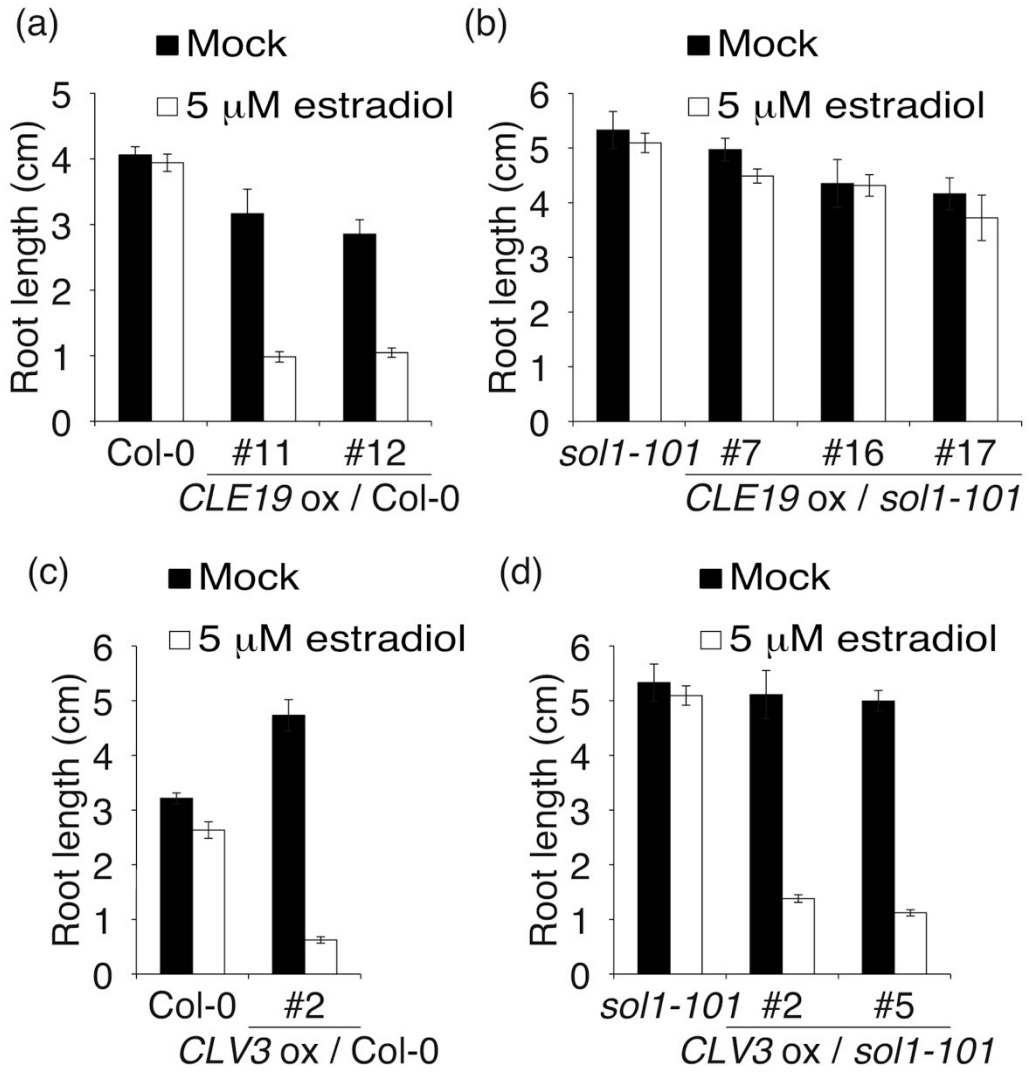

Figure 3-9. Effects of estrogen-induced *CLV3* and *CLE19* expression on root growth of the *sol1-101* mutant

(a) Primary root length of Col-0 plants overexpressing *CLE19* (n=10~11; mean ± SEM).

(b) Primary root length of *sol1-101* plants overexpressing *CLE19* (n=10~11; mean ± SEM).

(c) Primary root length of Col-0 plants overexpressing *CLV3* (n=10~11; mean ± SEM).

(d) Primary root length of *sol1-101* plants overexpressing *CLV3* (n=10~11; mean ± SEM).

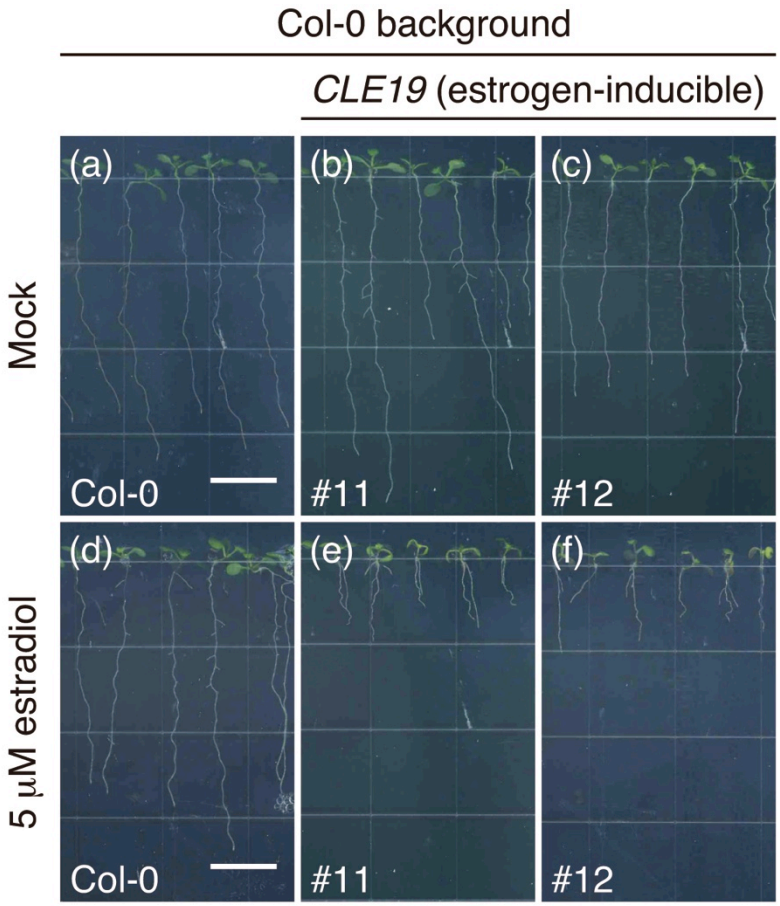

Figure 3-10. Effects of *CLE19* overexpression on Col-0
Col-0 (a, d), and Col-0 background (b, c, e, f) transgenic plants carrying estrogen-inducible *CLE19* were grown on 1/2 MS agar plates containing 5 μM β-estradiol or 0.05 % DMSO (Mock) for 9 days.
(a)-(c) Mock treatment. (d)-(f) 5 μM β-estradiol treatment.
Scale bars = 1 cm.

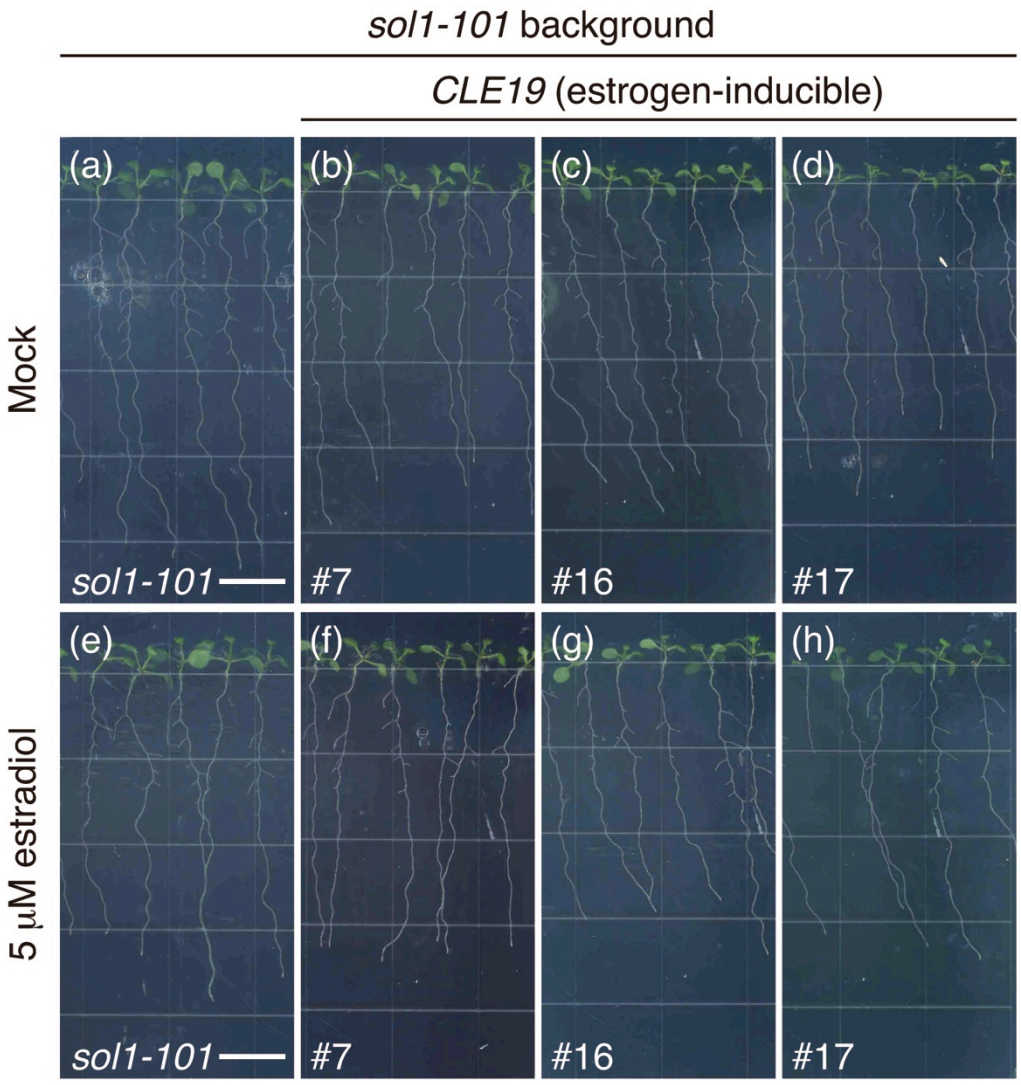

Figure 3-11. Effects of *CLE19* overexpression on *sol1-101*
sol1-101 (a, e), and *sol1-101* background (b, c, d, f, g, h) transgenic plants carrying estrogen-inducible *CLE19* were grown on 1/2 MS agar plates containing 5 μM β-estradiol or 0.05 % DMSO (Mock) for 9 days.
(a)-(d) Mock treatment. (e)-(h) 5 μM β-estradiol treatment.
Scale bars = 1 cm.

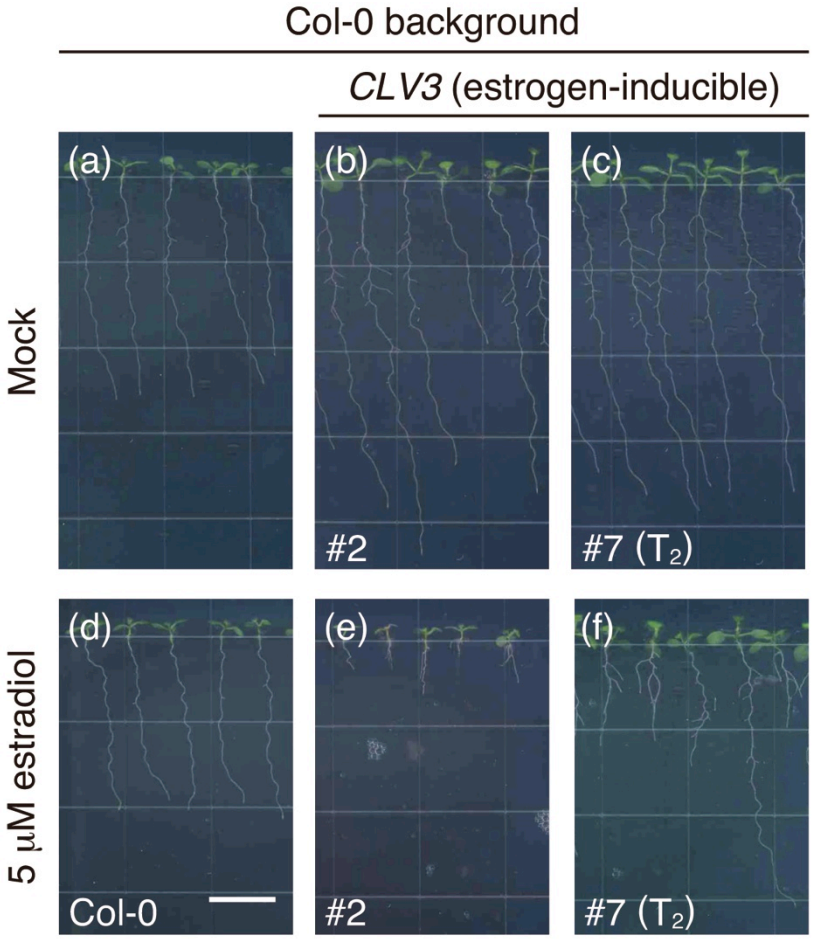

Figure 3-12. Effects of *CLV3* overexpression on Col-0
Col-0 (a, d) and Col-0 background (b, c, e, f) transgenic plants carrying estrogen-inducible *CLV3* were grown on 1/2 MS agar plates containing 5 μM β-estradiol or 0.05 % DMSO (Mock) for 9 days. #7 (c, i) is T2 generation.
(a)-(c) Mock treatment. (d)-(f) 5 μM β-estradiol treatment.
Scale bars = 1 cm.

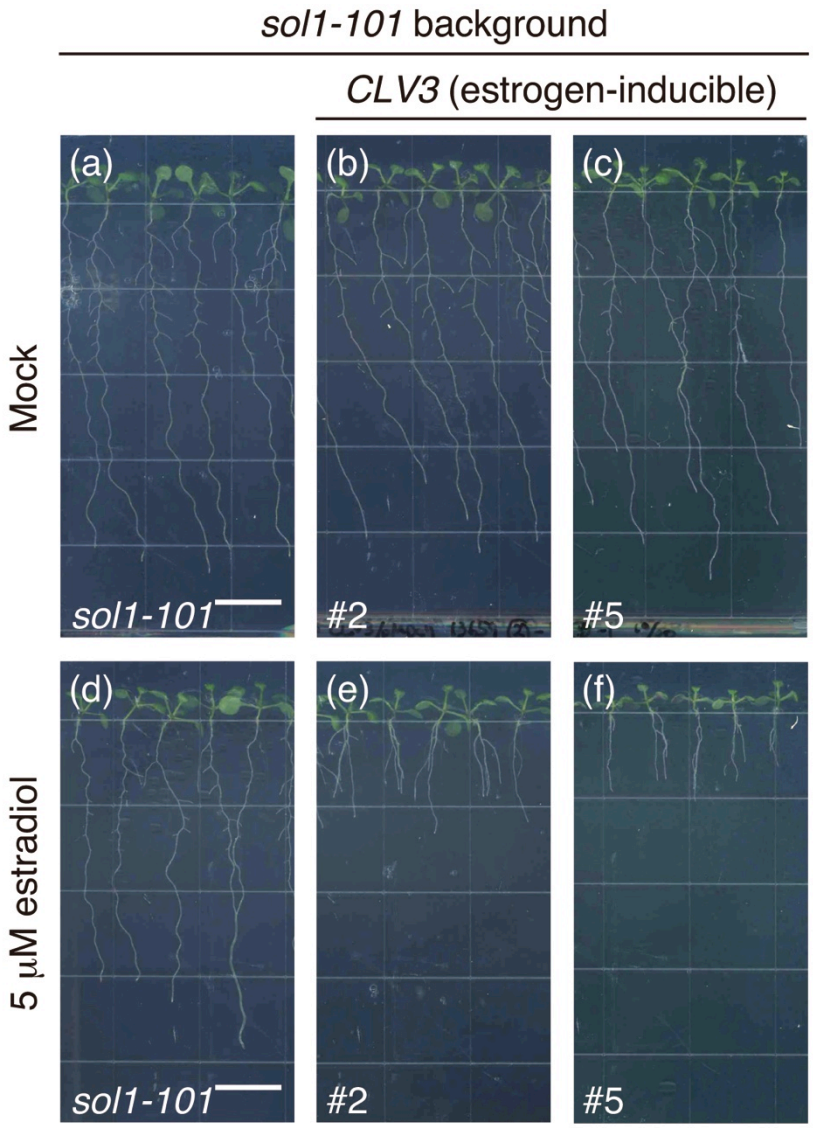

Figure 3-13. Effects of *CLV3* overexpression on *sol1-101*
sol1-101 (a, d) and *sol1-101* background (b, c, e, f) transgenic plants carrying estrogen-inducible *CLV3* were grown on 1/2 MS agar plates containing 5 μM β-estradiol or 0.05 % DMSO (Mock) for 9 days.
(a)-(c) Mock treatment. (d)-(f) 5 μM β-estradiol treatment.
Scale bars = 1 cm.

Table 3-1. Effects of the *sol1* mutation on carpel number

genotype	carpels per flower	SE	*n*
Col-0	2.00	0.00	100
sol1-101	2.00	0.00	100
sol1-102	2.00	0.00	100
rpk2-2	2.35	0.06	100
sol1-101 rpk2-2	2.17	0.04	100
clv1-101	3.03	0.08	100
sol1-101 clv1-101	3.00	0.08	80
clv2-101	2.46	0.06	100
sol1-101 clv2-101	2.42	0.06	100
clv3-8	4.14	0.10	100
sol1-101 clv3-8	4.26	0.10	100

The number of carpels in the 10 basal flowers of the inflorescence stem was counted.

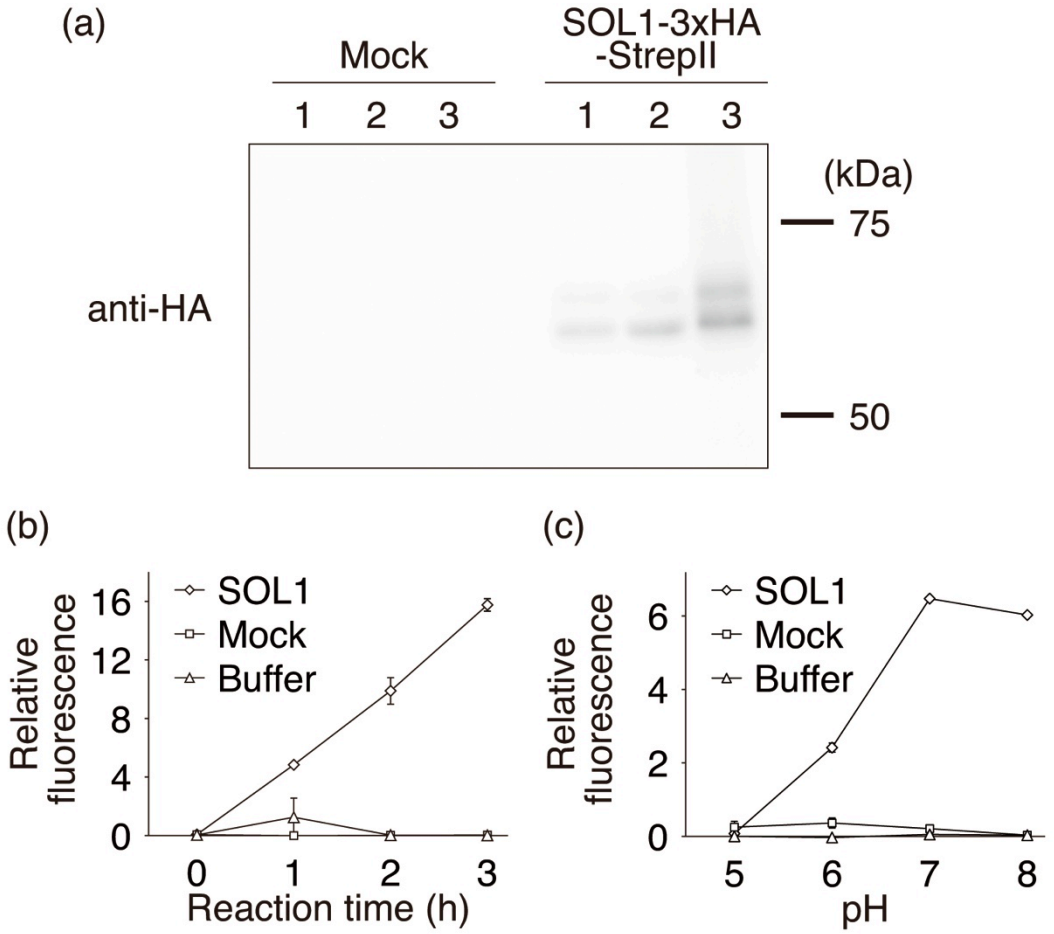

Figure 3-14. Carboxypeptidase activity of SOL1 on a fluorescent substrate
(a) Immunoblot assay of affinity-purified SOL1-3HS. 1: Total extract; 2: Flow-through; 3: Purified protein.
(b) Enzymatic activity of the purified fractions on Dansyl-Phe-Ala-Arg. The relative fluorescence of Dansyl-Phe-Ara, a reaction product, was detected. Reactions were performed for the indicated time periods at 30ºC, pH7.0 (n=3; mean ± SEM).
(c) pH-dependent enzymatic activity of SOL1-3HS on Dansyl-Phe-Ala-Arg. The relative fluorescence of Dansyl-Phe-Ara was measured. Reactions were performed for 3 h at 30ºC at the indicated pH levels. (n=3; mean ± SEM).

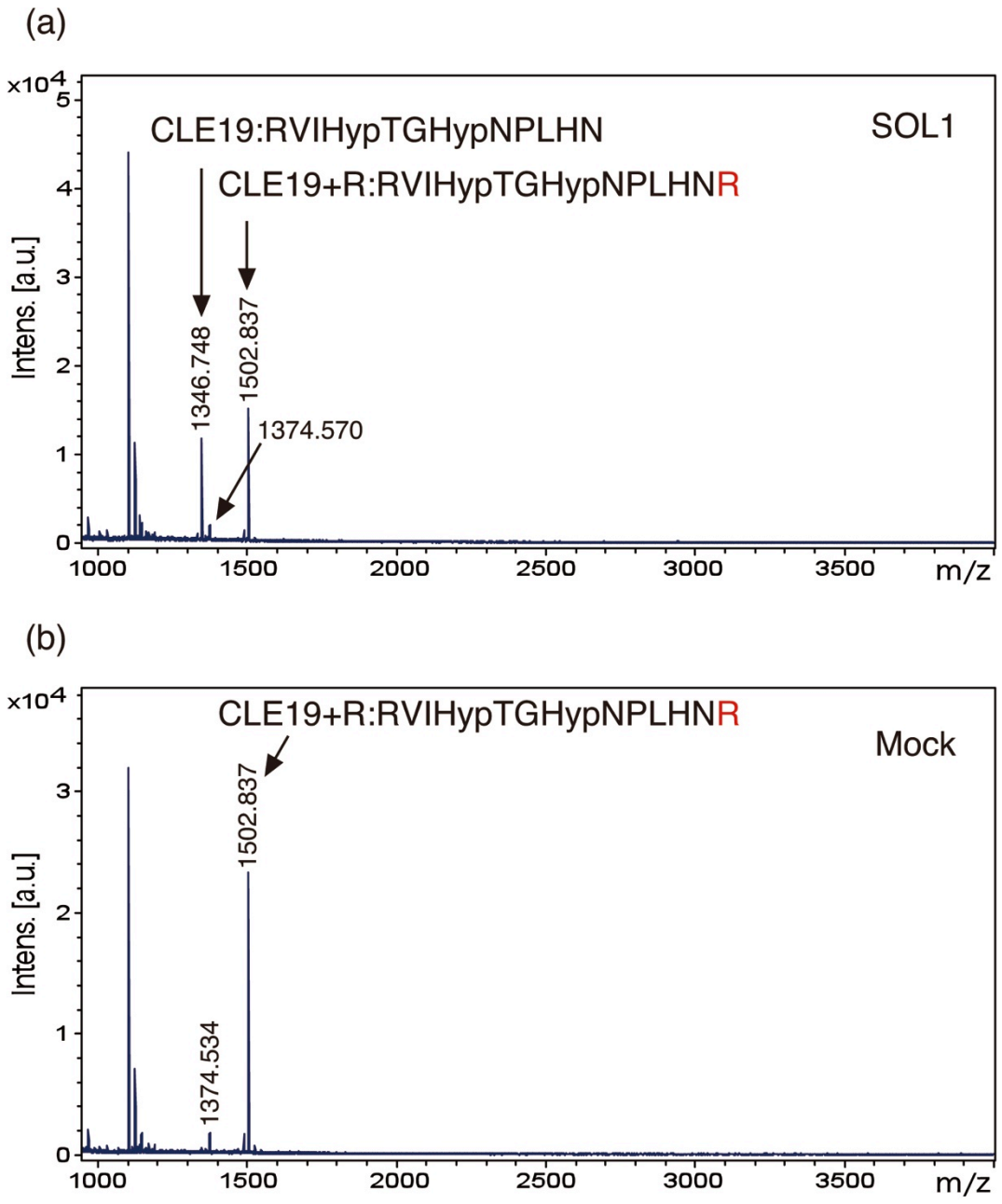

Figure 3-15. Carboxypeptidase activity of SOL1 on the C-terminal arginine of CLE19+R peptide
(a) Reaction of SOL1 with CLE19+R. (b) Mock reaction of CLE19+R.

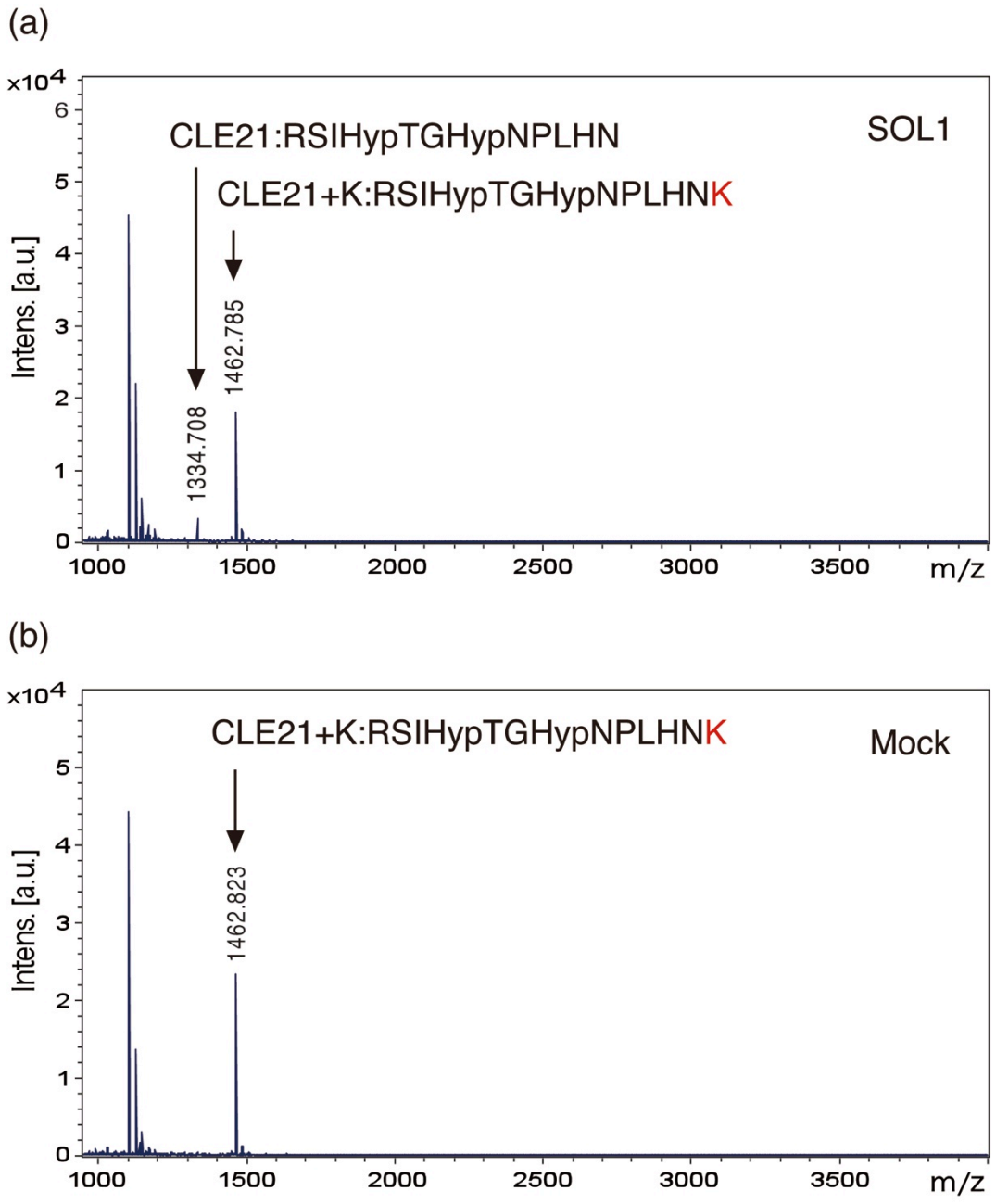

Figure 3-16. Carboxypeptidase activity of SOL1 on the C-terminal lysine of CLE21+K peptide
(a) Reaction of SOL1 with CLE21+K. (b) Mock reaction of CLE21+K.

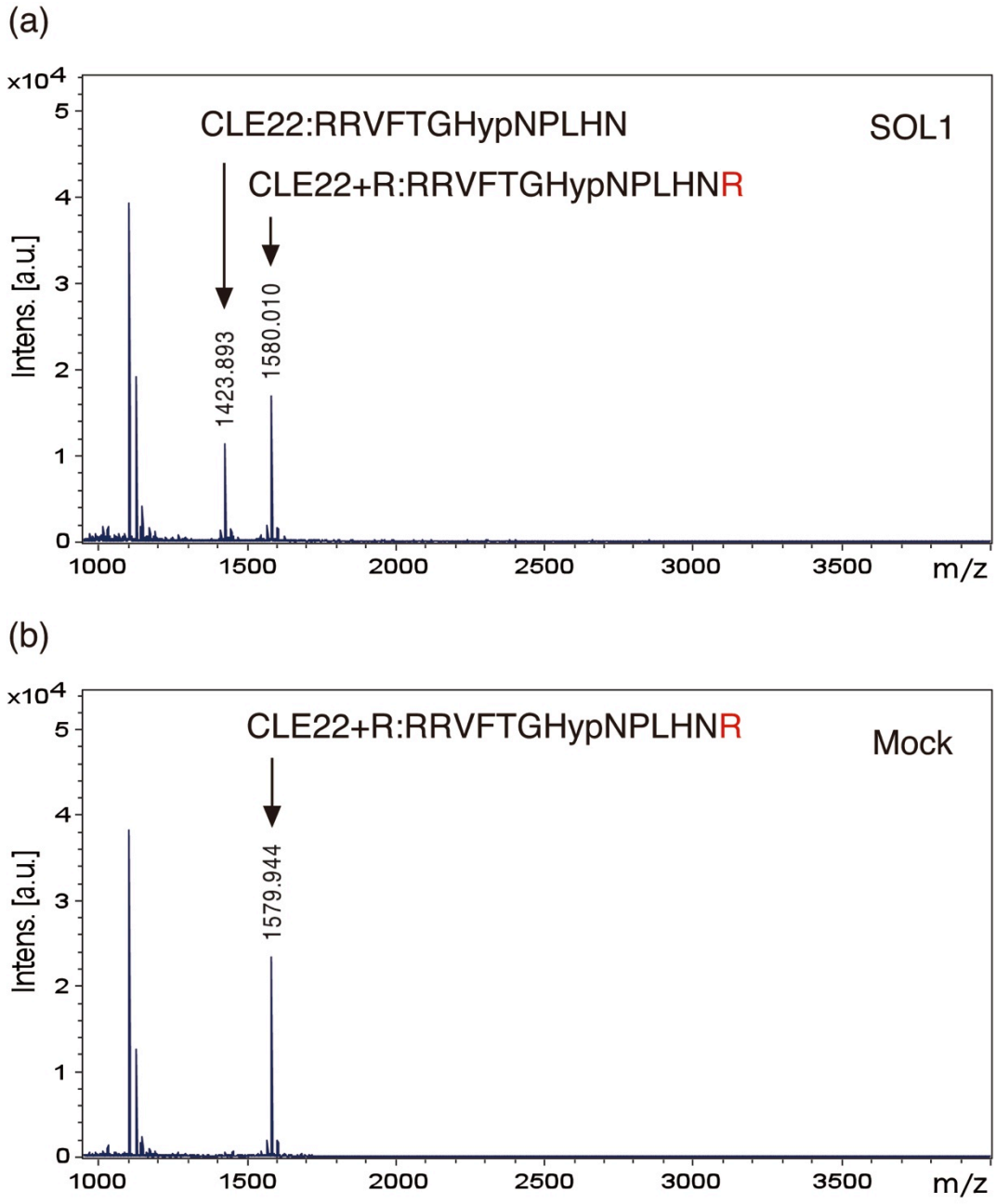

Figure 3-17. Carboxypeptidase activity of SOL1 on the C-terminal arginine of CLE22+R peptide
(a) Reaction of SOL1 with CLE22+R. (b) Mock reaction of CLE22+R.

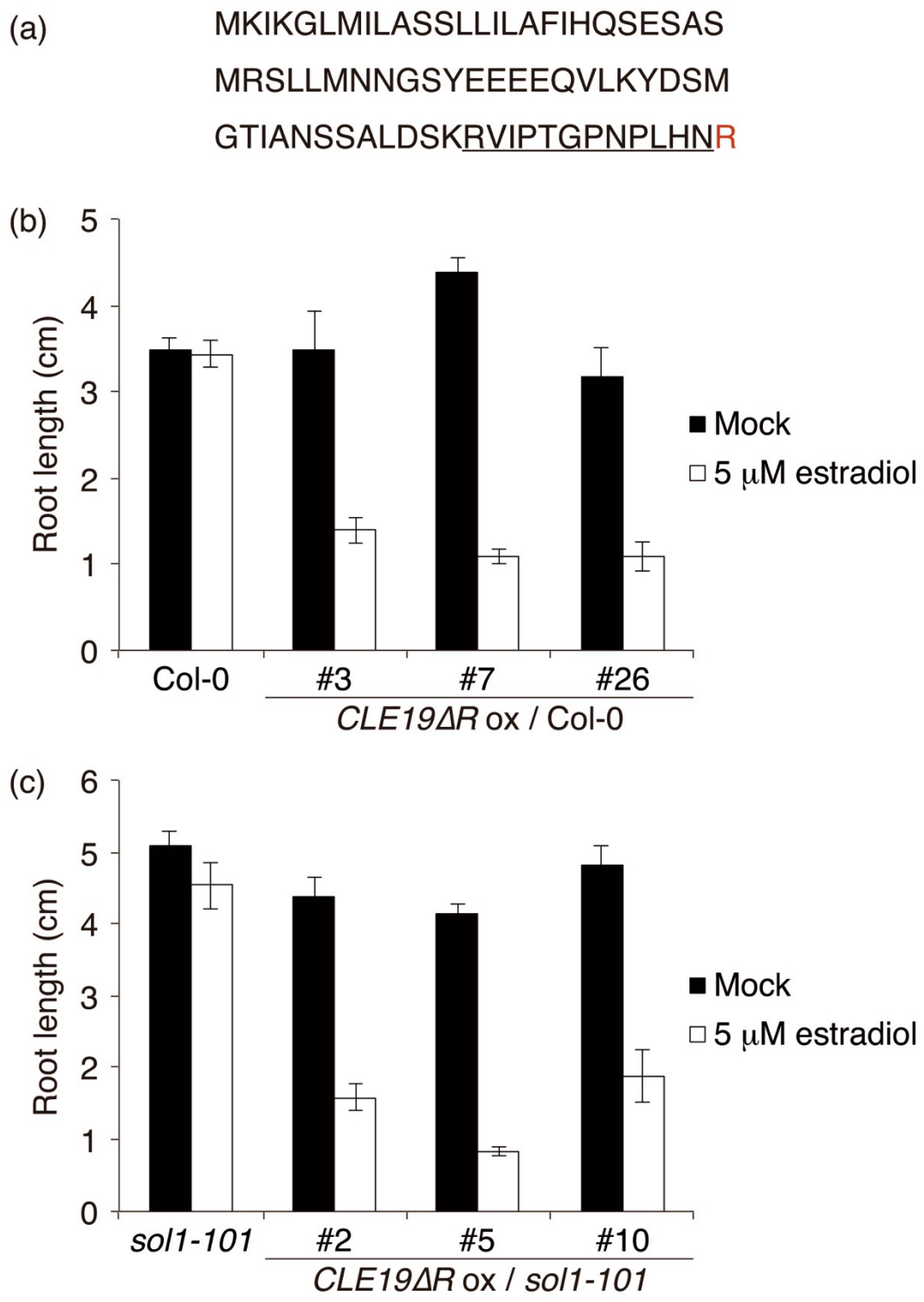

Figure 3-18. Effects of estrogen-induced *CLE19ΔR* expression on Col-0 and *sol1-101*
(a) The full-length amino acid sequence of CLE19. The CLE domain is underlined. R (in red) indicates the C-terminal arginine residue that is absent in CLE19ΔR.
(b) Primary root length of Col-0 plants overexpressing *CLE19ΔR* (n=8~11; mean ± SEM).
(c) Primary root length of *sol1-101* plants overexpressing *CLE19ΔR* (n=9~11; mean ± SEM).

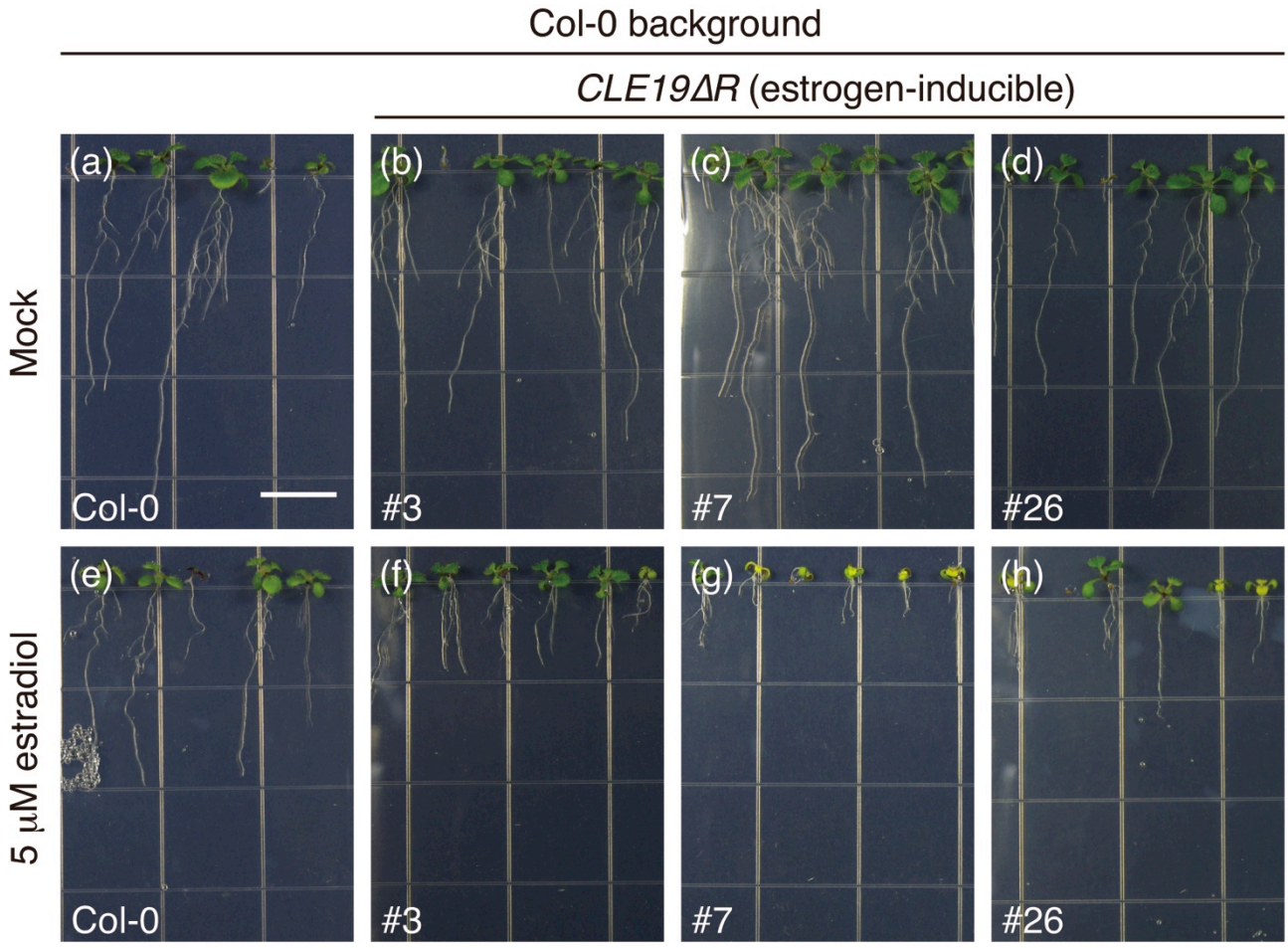

Figure 3-19. Effects of *CLE19ΔR* overexpression on Col-0
Col-0 (a, e) and Col-0 background (b, c, d, f, g, h) transgenic plants carrying estrogen-inducible *CLE19ΔR* were grown on 1/2 MS agar plates containing 5 μM β-estradiol or 0.05 % DMSO (Mock) for 9 days.
(a)-(d) Mock treatment. (e)-(h) 5 μM β-estradiol treatment.
Scale bars = 1 cm.

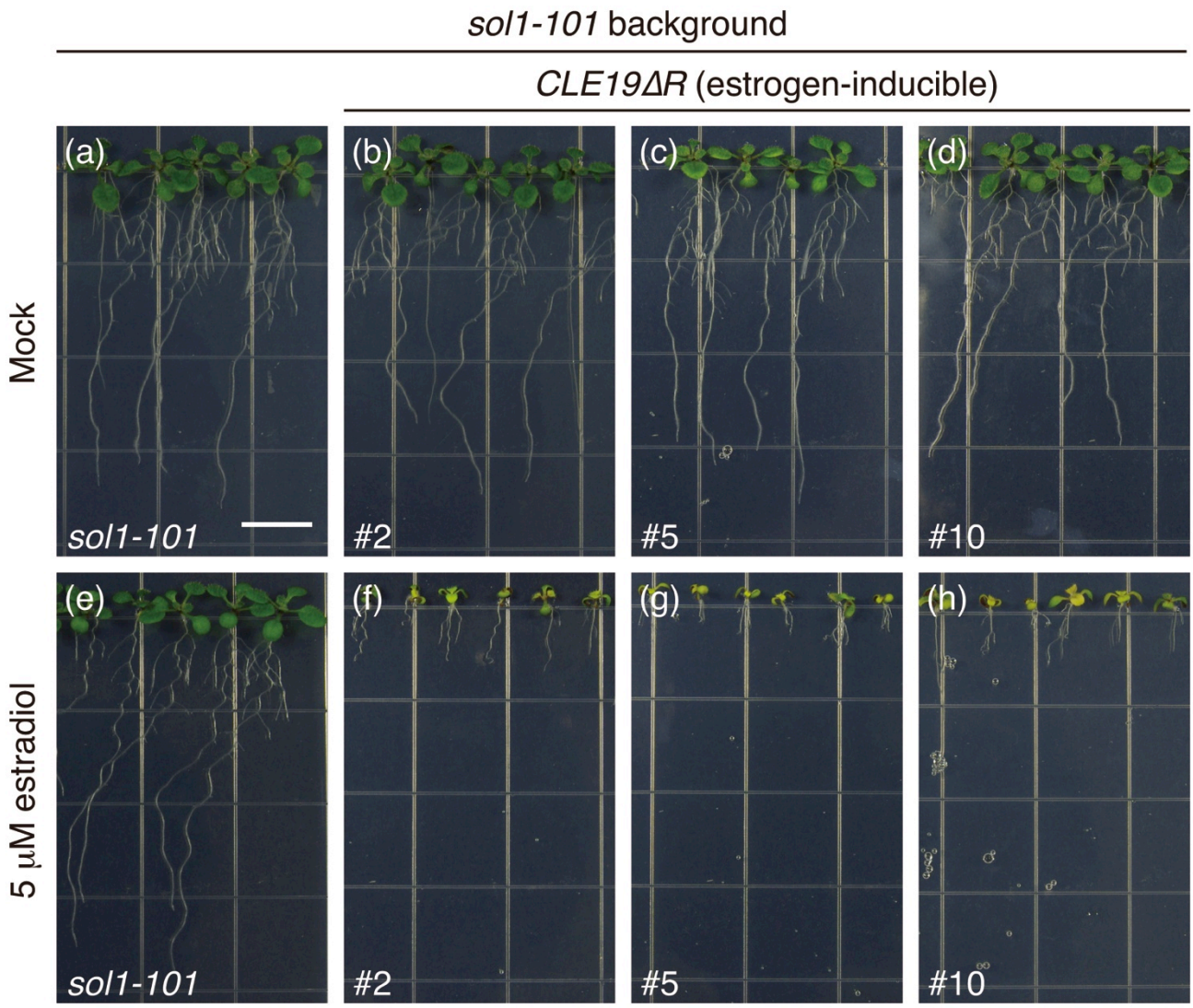

Figure 3-20. Effects of *CLE19ΔR* overexpression on *sol1-101*
sol1-101 (a, e) and *sol1-101* background (b, c, d, f, g, h) transgenic plants carrying estrogen-inducible *CLE19ΔR* were grown on 1/2 MS agar plates containing 5 *μ*M β-estradiol or 0.05 % DMSO (Mock) for 9 days.
(a)-(d) Mock treatment. (e)-(h) 5 *μ*M β-estradiol treatment.
Scale bars = 1 cm.

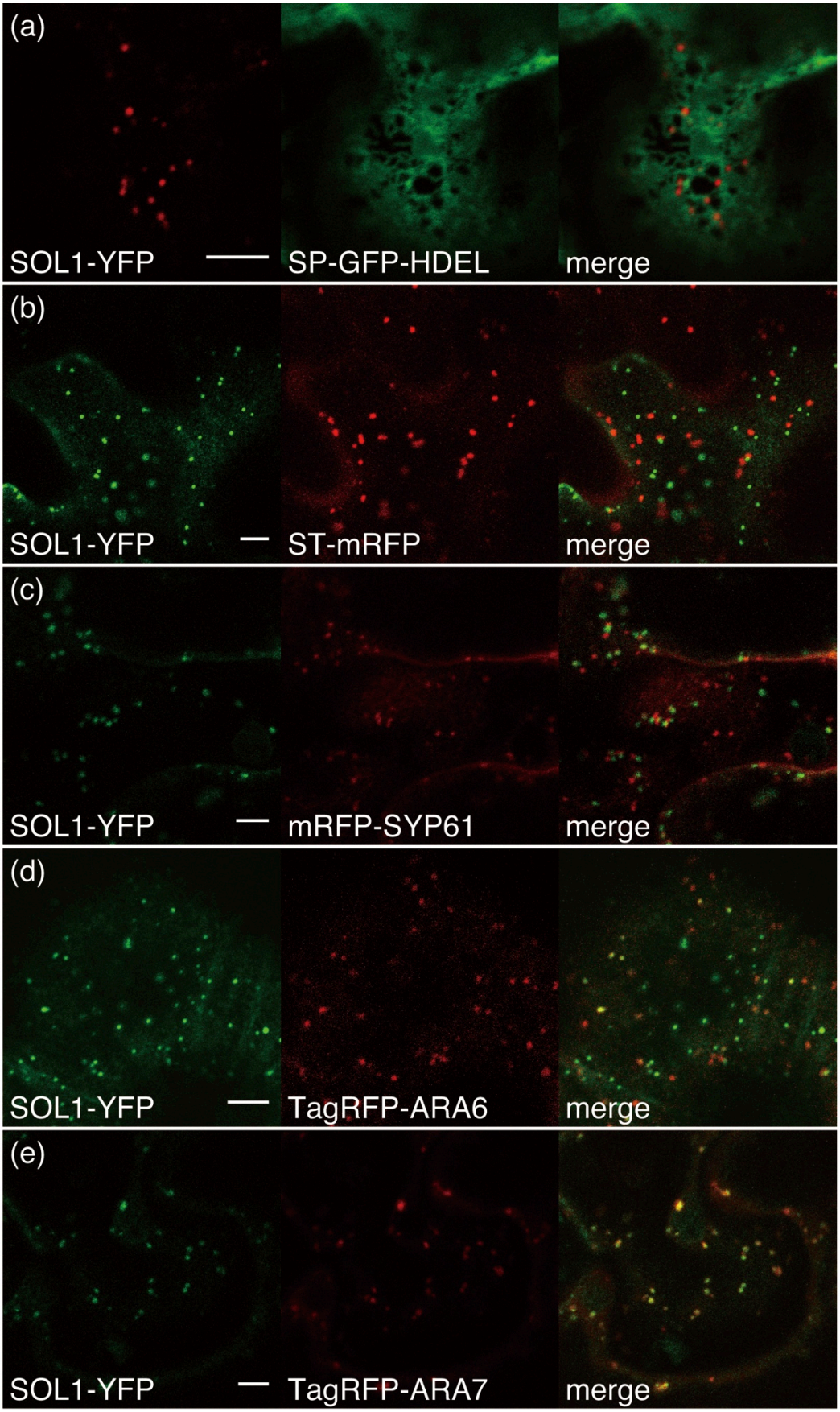

Figure 3-21. Subcellular localization of SOL1-YFP and organelle markers transiently expressed in *N. benthamiana* leaves
SOL1-YFP was transiently coexpressed with (a) SP-GFP-HDEL, (b) ST-mRFP, (c) mRFP-SYP61, (d) TagRFP-ARA6 and (e) TagRFP-ARA7.
Scale bars = 5 μm.

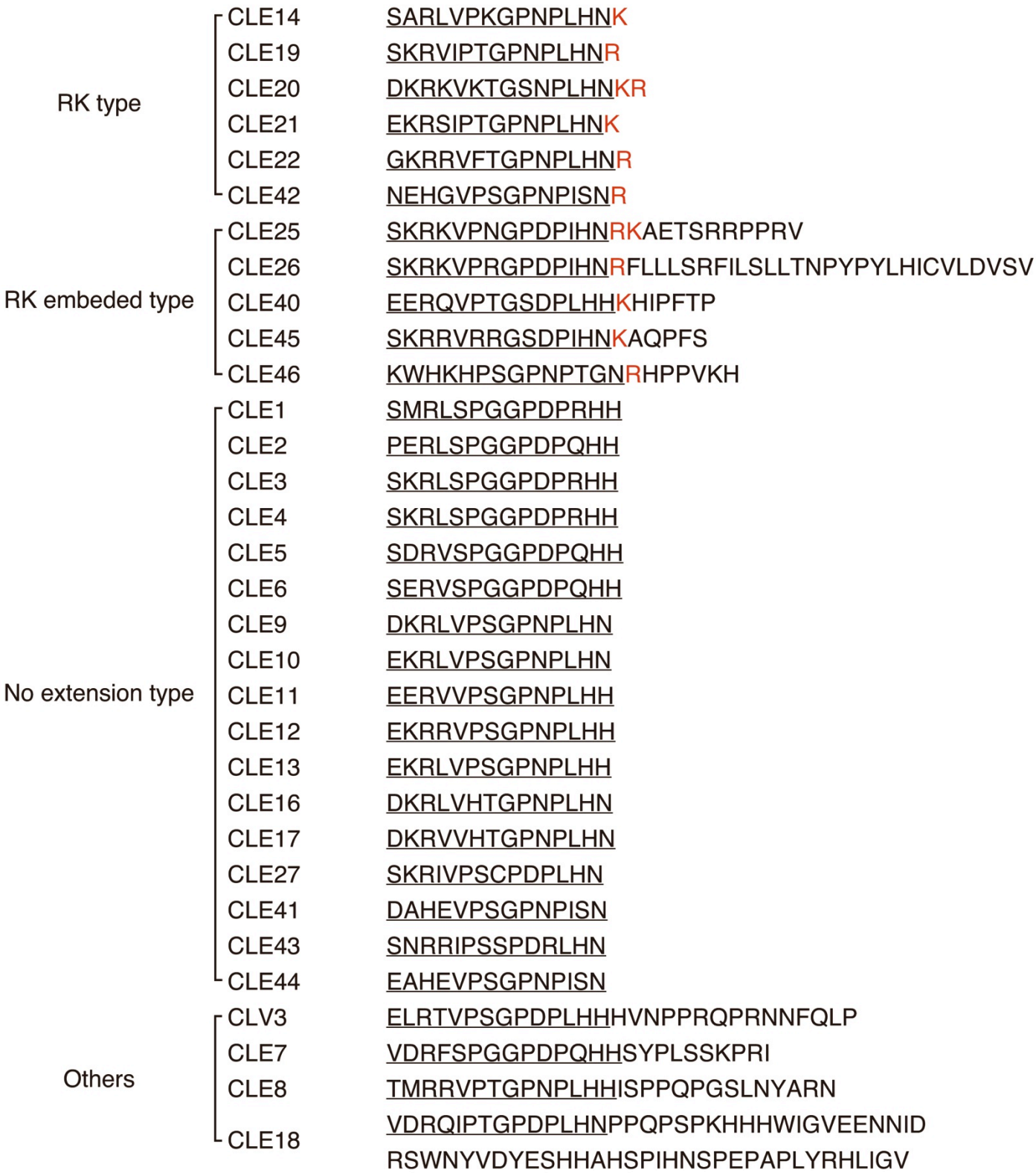

Figure 3-22. C-terminal sequences of CLE peptides
C-terminal sequences of *Arabidopsis thaliana* CLE peptides are indicated from conserved CLE domain. CLE domains are underlined and red characters indicate possible target sites of SOL1.

Chapter IV: Analysis of downstream factors of CLE peptides

Introduction

WOX genes encode homeodomain transcription factors playing important roles in development of various tissues in plants. For example, *WOX2*, *WOX8* and *WOX9* are involved in apical-basal patterning in embryos and *WOX3/PRESSED FLOWER* (*PRS*) and *WOX1* are involved in leaf blade outgrowth and adaxial/abaxial patterning of leaf margin tissues (Haecker *et al.*, 2004; Breuninger *et al.*, 2008; Vandenbussche *et al.*, 2009; Nakata *et al.*, 2012). Besides, it is known that *WUS*, *WOX4* and *WOX5,* which function downstream of CLE peptides, promote stem cell proliferation in the shoot apical meristem, the vascular meristem and the root apical meristem, respectively (Stahl *et al.*, 2009; Hirakawa *et al.*, 2010; Yadav *et al.*, 2010).

There are 15 *WOX* genes in *A. thaliana.* WUS functions both as transcriptional activator and repressor (Lohmann *et al.*, 2001; Leibfried *et al.*, 2005). WOX proteins contain a conserved homeodomain. In addition to the domain, WUS has another functional region, called WUS box, which is located downstream of the homeodomain and conserved in WOX1-WOX7 and WUS (Ikeda *et al.*, 2009). An analysis of WUS with a mutated WUS box revealed that the WUS box is crucial for transcriptional activity of WUS (Ikeda *et al.*, 2009). Comprehensive analysis revealed direct targets of WUS such as *AGAMOUS* (*AG*), *ARABIDOPSIS RESPONSE REGULATOR 7* (*ARR7*), *CLAVATA1* (*CLV1*), *TOPLESS* (*TPL*), *TOPLESS-RELATED 1* (*TPR1*), and *TPR2,* which contributed to the understanding function of WUS *in situ* (Lohmann *et al.*, 2001; Leibfried *et al.*, 2005; Busch *et al.*, 2010). However, the downstream targets of other

WOX genes are still unknown and then molecular functions of *WOX* genes involved in CLE signaling remains to be solved.

Vascular tissues are continuously produced by proliferation and differentiation of vascular stem cells in the vascular meristem. It is considered that strict regulation of balance between stem cell proliferation and differentiation is critical for function of vascular tissues. A physiological experiment using *Zinnia* cell culture system identified TRACHEARY ELEMENT DIFFERENTIATION INHIBITORY FACTOR (TDIF), a CLE peptide secreted from phloem, as an important factor involved in vascular stem cell regulation (Ito *et al.*, 2006; Hirakawa *et al.*, 2008). TDIF is perceived by TDIF receptor (TDR), which is expressed in the vascular stem cells, to simultaneously inhibit xylem differentiation and promote their own proliferation (Hirakawa *et al.*, 2008; Hirakawa *et al.*, 2010). WOX4 promotes TDIF-dependent vascular stem cell proliferation (Hirakawa *et al.*, 2010). An important remaining issue is to reveal how WOX4 functions in this regulation.

For this purpose, I tried to identify downstream genes of WOX4 in relation to vascular stem cell proliferation. In this analysis, I also used WUS as a control to compare with downstream genes of WOX4. To take advantage of homogenous and abundant sample collection and simultaneous induction of transgenes, I established transgenic *Arabidopsis* cell culture systems harboring an inducible *WOX4* or *WUS*. This is because transgenic *Arabidopsis* cultures have been successfully used for searching downstream factors of VASCULAR-RELATED NAC-DOMAIN 6 (VND6), a transcription factor regulating metaxylem vessel differentiation (Oda *et al.*, 2010;

Ohashi-Ito *et al.*, 2010). Using these cultures, I comprehensively searched genes whose expression rapidly respond to induction of *WOX4* with microarray. As a result, I succeeded in identification of candidates that may function downstream of *WOX4*.

Results

Functional characterization of WOX4-ECFP *in vivo*

In order to reveal downstream genes of *WOX4*, I planned to identify genes rapidly up- or down-regulated by *WOX4* using microarray analysis. For following the behavior of the WOX4 protein, Enhanced Cyan Fluorescent Protein was fused to the C-terminus of WOX4 (WOX4-ECFP). To examine whether WOX4-ECFP is functional *in planta* or not, the *wox4-1* mutant, a loss-of-function mutant of *WOX4*, was transformed with $WOX4_{pro}$*:WOX4-ECFP,* which is a construct composed of *WOX4-ECFP*, the own promoter of *WOX4* (3 kbp upstream sequence from *WOX4* translational start site), and 1.5 kbp downstream sequence from *WOX4* translational stop site. T3 *wox4-1* transgenic plants harboring homozygous $WOX4_{pro}$*:WOX4-ECFP*, wild-type plants and *wox4-1* mutants were subjected to phenotypic analysis of procambial cell proliferation in hypocotyls. Hypocotyls from seedlings grown for 16 days with or without 1 μM TDIF were sectioned and analyzed for procambial cell proliferation. As expected, introduction of $WOX4_{pro}$*:WOX4-ECFP* into *wox4-1* mutants increased the number of procambial cell layers as much as that of wild-type (Figure 4-1a-c). Furthermore, TDIF sensitivity was examined and *wox4-1* mutants did not show TDIF dependent-promotion of procambial cell proliferation as previously reported (Hirakawa *et al.*, 2010). By contrast, *wox4-1* transgenic plants expressing *WOX4-ECFP* exhibited xylem vessels intercalated with ectopically proliferated cells as observed in wild-type (Figure 4-1). These results indicate that WOX4-ECFP is functional *in planta*.

Production of transgenic *Arabidopsis* cell cultures expressing estrogen-inducible *WOX4-ECFP* and *WUS-ECFP*

Since WOX4-ECFP was revealed to be functional *in planta*, I tried to produce transgenic *Arabidopsis* cell cultures expressing *WOX4-ECFP* and also cultures expressing *WUS-ECFP* or *ECFP* as controls. For simultaneous induction, these transgenes were put under the control of estrogen-inducible promoter. An *Arabidopsis* cell culture, Alex, which has been established from *A. thaliana* (Col-0 background) root explants, was transformed through co-cultivation with *R. radiobacter* carrying these constructs (Mathur *et al.*, 1998). Then, after killing bacteria with Claforan, cell cultures were subcultured at a one-week interval with continuous addition of hygromycin B for selection of transgenic cells. At least 6 subcultures were performed before carrying out subsequent experiments.

Characterization of estrogen-induced expression of transgenes in the transgenic *Arabidopsis* cell cultures

I examined time course of estrogen-induced gene expression in the transgenic cell cultures established above. Transgenic cells were grown for 5 days after subculture, and then β-estradiol was added to the cultures at a final concentration of 5 μM. Cells were collected 0, 1, 2, 3, 4, 5 and 6 h after estrogen addition and examined for transgene expression with qRT-PCR. Expression levels of both *WOX4-ECFP* and *WUS-ECFP* were rapidly and conspicuously increased to more than 100 times at 3 h and to more than 300 times at 6 h (Figure 4-2). Microscopic observation of ECFP fluorescence was

also made for cells that were treated with 5 μM β-estradiol for 24 h. ECFP fluorescence was detected only in nuclei in *WOX4-ECFP*- and *WUS-ECFP*-expressing cells, but in the cytoplasm in *ECFP*-expressing cells (Figure 4-3). These results indicate that estrogen can induce rapidly and efficiently *WOX4-ECFP* and *WUS-ECFP,* whose products accumulate in nuclei as transcription factors.

Investigation of downstream genes of *WOX4* using microarray analysis

Because I succeeded in producing *Arabidopsis* cell cultures in which estrogen induces *WOX4-ECFP* and *WUS-ECFP* rapidly and efficiently, next I performed microarray analyses using these cultures. Five-day-old transgenic cell cultures harboring estrogen-inducible *WOX4-ECFP*, *WUS-ECFP* and *ECFP* were treated with 5 μM β-estradiol to induce transgene expression, and treated cells were collected at 0 h and 6 h. RNAs were purified from these cells and subjected to microarray analyses. Distribution of individual gene expression levels obtained from microarray analyses were well approximated by logarithmic normal distribution, and therefore these data were log2-transformed for further statistical analysis (Hoyle *et al.*, 2002). The comparison of gene expression between *ECFP* expressing cells and *WOX4-ECFP* or *WUS-ECFP* expressing cells displayed *WOX4*-related genes and *WUS*-related genes (Table 4-1). *WOX4-ECFP* expression preferentially up-regulated 95 genes and down-regulated 129 genes. *WUS-ECFP* expression preferentially up-regulated 223 genes and down-regulated 116 genes. In addition to them, 36 genes are up- or down-regulated by both *WOX4-ECFP* and *WUS-ECFP* expression. Interestingly, all

except one, which is down-regulated by *WOX4-ECFP* and up-regulated in *WUS-ECFP,* are up- or down-regulated commonly by both of *WOX4-ECFP* and *WUS-ECFP*. Because WUS is known to function as both an inducer and a repressor of gene expression, this result suggests that WOX4 also has both activities (Lohmann *et al.*, 2001; Leibfried *et al.*, 2005; Ikeda *et al.*, 2009; Busch *et al.*, 2010).

Genes up- or down-regulated by *WOX4-ECFP* induction were implicated to encode proteins with various functions: transcriptional factors, ligands, receptors, micro RNAs, transporters, enzymes and so on. Among them, I focused on genes that showed a larger expression change and are predicted to function in transcriptional regulation; *at1g01183* (*mir165a*), *at1g28360* (*erf12*), *at3g15210* (*erf4*), *at4g20880* (*ert2*), *at5g64800* (*cle21*) and *at3g17600* (*iaa31*) (Table 4-2). I collected T-DNA insertion mutants of them, from the Arabidopsis Biological Resource Center (www.abrc.osu.edu) at Ohio State University (Diévart *et al.*, 2003) and established homozygous mutant lines. To understand their function in vascular development, I performed phenotypic observation in hypocotyls. However, these mutants showed no obvious difference in vascular stem cell proliferation in hypocotyl sections of seedlings grown for 16 days from wild-type (Figure 4-4).

Discussion

WOX4-ECFP and WUS-ECFP function as transcription factors in transgenic *Arabidopsis* cell cultures

In this study, transgenic *Arabidopsis* cell cultures expressing *WOX4-ECFP*, *WUS-ECFP* and *ECFP* under the control of the estrogen-inducible promoter were produced for investigating transcriptional regulation of WOX4 and WUS. Estrogen treatment rapidly and conspicuously induced *WOX4-ECFP* and *WUS-ECFP* expression in the cell cultures. This rapid and conspicuous induction of *WOX4-ECFP* and *WUS-ECFP* was considered to allow me to identify genes regulated directly by WOX4 or WUS. Moreover, nuclear localization of WOX4-ECFP and WUS-ECFP in the transgenic cells is consistent with their function as transcription factors and actually WOX4-ECFP could function as a transcription factor *in situ,* when judged from the fact that *WOX4-ECFP* rescues the defect in vascular stem cell proliferation in the *wox4-1* mutant. The induction of *WOX4-ECFP* and *WUS-ECFP* in cultured cells caused rapid changes in gene expression profiles, which supports my idea that *WOX4-ECFP* and *WUS-ECFP* function as transcription factors even in cultured cells.

Transgenic *Arabidopsis* cell cultures as a useful tool for investigating downstream factors of WOX4 and WUS

Having confirmed functions of WOX4-ECFP and WUS-ECFP as transcription factors, I searched genes that were up- or down-regulated by these transcription factors in microarray analysis and found a number of genes up- or down-regulated in

WOX4-ECFP and *WUS-ECFP*-dependent manners. Busch and others analyzed gene expression profiles in vegetative shoot apical meristems and influorescence meristems of *A. thaliana* under *WUS*-overexpression and *CLV3*-oveerexpression with microarrays and identified 675 genes as *WUS* response genes (Busch *et al.*, 2010). Of them, 28 genes were overlapped with *WUS*-related genes I selected in this study. Although much larger amount of genes was obtained as WUS-related genes in both the microarray data from Busch and others and mine, they were not selected as common genes. Data from Busch and others are a mixture of data from various experiments with different meristems, *clv3* mutants and *CLV3* overexpressor as well as with *WUS* overexpressor and *wus* mutants (Busch *et al.*, 2010). Considering the mixed nature of genes reported by Busch and others, which includes *CLV3*-related genes that do not function downstream of WUS signaling and WUS-related genes expressed only in distinct differentiation stage, the low ratio of the common genes may be explicable.

Nevertheless, it is important that 28 genes are common as WUS-related genes and that most (22 of 28) of the common genes were similarly up- or down-regulated in both *in situ* and my culture. This fact indicates that, in spite of completely different cell backgrounds used in these experiments, these genes are regulated by *WUS* or *WUS-ECFP* in the same manner. Therefore, the *Arabidopsis* cell culture system harboring a transcription factor is useful to investigate, at least, a part of downstream pathways of the transcription factor. This conclusion is also consistent with the previous results from *Arabidopsis* cell culture in which *VND6* and *SND1* is induced (Oda *et al.*, 2010; Ohashi-Ito *et al.*, 2010). Similarly, an *Arabidopsis* culture harboring an inducible

WOX4-ECFP is expected to be useful for identifying its downstream genes. Further characterization of candidate downstream genes will verify value of this system as a useful tool for downstream gene investigation.

WOX4 function is largely different from WUS

Microarray analysis indicated only limited overlap between *WOX4*-related genes and *WUS*-related genes, most of which were specific to the respective transgenes. This result suggests that WOX4 function may be largely different from that of WUS in spite of high conservation of their domain structure. Among WOX4-related genes, 3 genes (*ERF12*, *ERF4* and *ERT2*) were predicted to be involved in ethylene signaling. Ethylene is involved in tension wood formation by promoting cell division in the vascular meristem (Love *et al.*, 2009). Exogenous application of 1-aminocyclopropane -1-carboxylate, ethylene precursor, increases cell division as well as over-production of endogenous ethylene (Love *et al.*, 2009; Etchells *et al.*, 2012). Therefore, detailed analysis of mutants of these genes focusing on ethylene signaling may reveal so far unknown relationship between WOX4-mediated vascular stem cell proliferation and ethylene signaling.

Mutants examined in this study including *erf12*, *erf4* and *ert2* did not show distinct vascular phenotype from wild-type. Genetic redundancy may mask defects in these mutants and analyses on multiple mutants are necessary to examine contribution of these genes to vascular development. I will also perform phenotypic observation of other *WOX4*-related gene mutants. In addition to genetic analyses, identification of

direct target genes of WOX4 through ChIP-Seq using transgenic *Arabidopsis* cell cultures and of binding sequence of WOX4 will help understanding of WOX4-dependent vascular stem cell proliferation. Furthermore, thorough investigations of common functions between WOX4 and WUS during plant development will provide useful information about common nature between the vascular meristem and the SAM, in particular, about CLE peptide dependent regulation of stem cells.

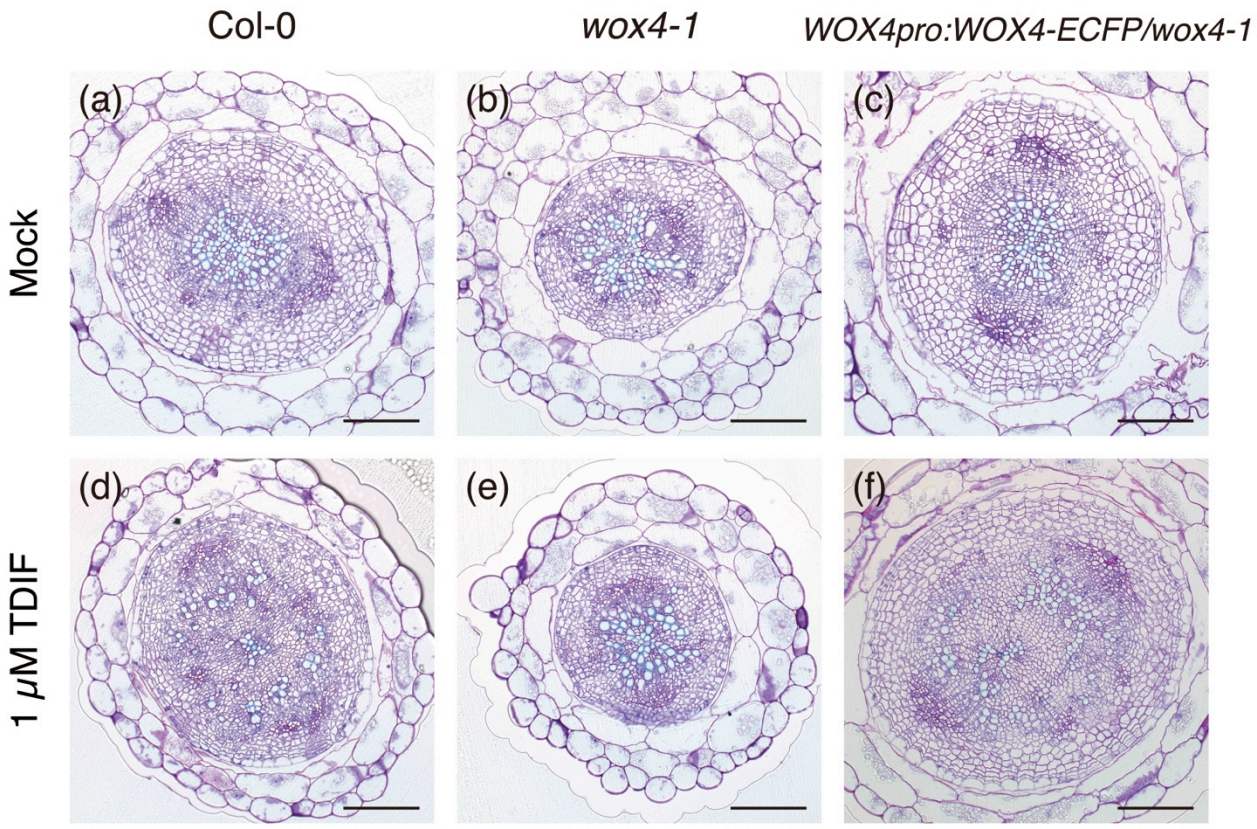

Figure 4-1. Hypocotyl sections of seedlings treated with TDIF
Col-0 (a, d), *wox4-1* (b, e) and *WOX4*$_{pro}$*:WOX4-ECFP/wox4-1* (c, f) plants were grown on 1/2 MS agar plates containing TDIF peptide for 16 days.
(a)-(c) Mock treatment. (d)-(f) 1 μM TDIF treatment.
Scale bars = 100 μm.

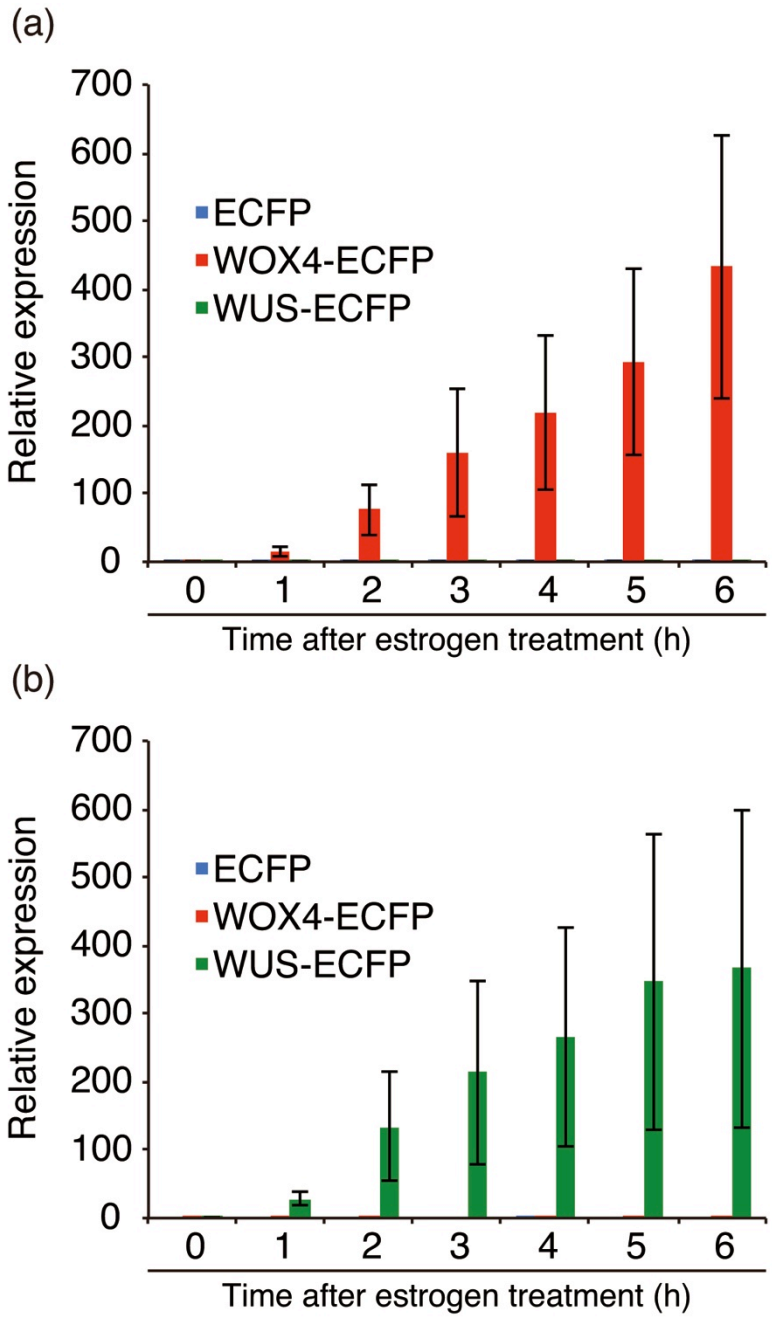

Figure 4-2. Estrogen-inducible expression of transgenes
Five-day-old transgenic cells harbouring estrogen-inducible *WOX4-ECFP*, *WUS-ECFP* and *ECFP* were treated with 5 μM β-estradiol.
(a) Expression of *WOX4*. (b) Expression of *WUS*.

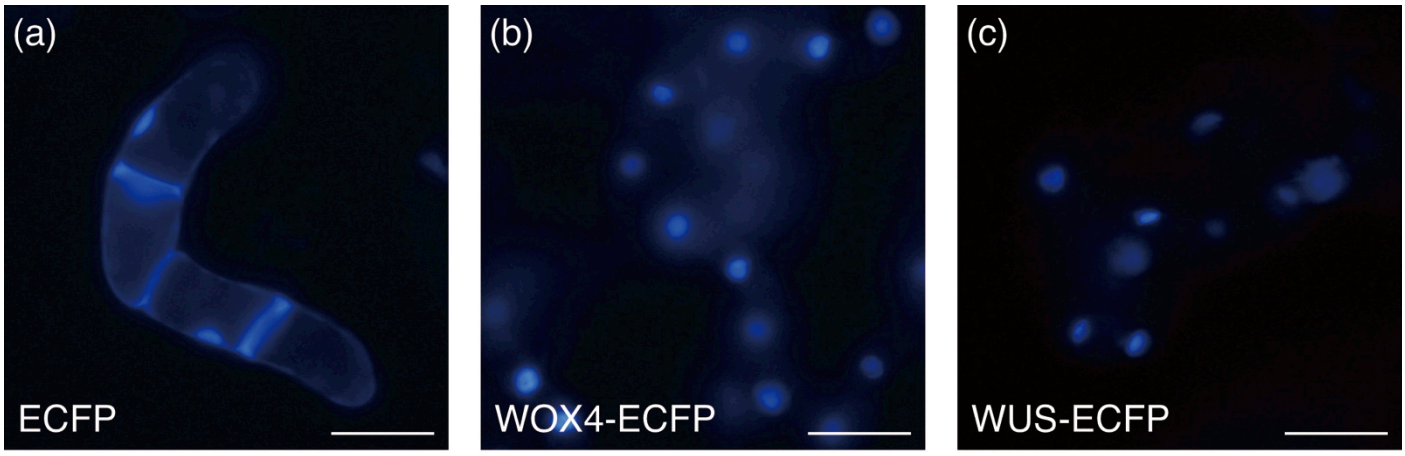

Figure 4-3. Subcellular localization of ECFP, WOX4-ECFP and WUS-ECFP.
Five-day-old transgenic cells were treated with 5 μM β-estradiol for 24 h.
(a) ECFP. (b) WOX4-ECFP. (c) WUS-ECFP.
Scale bars = 50 μm.

Table 4-1. Genes up- or down-regulated by *WOX4* or *WUS*

	WOX4-specific	common	*WUS*-specific
upregulated	95	15	223
downregulated	129	20	116

Four times of biological replicates were performed for the analysis. Genes that showed statistically significant ($p<0.01$) expression change compared with ECFP were counted.

Table 4-2. Genes chosen for phenotypic analysis

Gene	Short description in TAIR10	log2 (fold change)
AT1G01183	MIR165/MIR165A	-1.09
AT3G21270	DOF zinc finger protein 2 (DOF2)	1.01
AT1G28360	ERF domain protein 12 (ERF12)	0.86
AT3G17600	indole-3-acetic acid inducible 31 (IAA31)	-0.61
AT5G64800	CLAVATA3/ESR-RELATED 21 (CLE21)	-0.54
AT4G36740	homeobox protein 40 (HB40)	-0.53
AT2G45680	TCP family transcription factor	0.52
AT4G20880	ethylene-responsive nuclear protein / ethylene-regulated nuclear protein (ERT2)	0.52
AT4G16780	homeobox protein 2 (HB-2)	0.49
AT3G15210	ethylene responsive element binding factor 4 (ERF4)	0.38

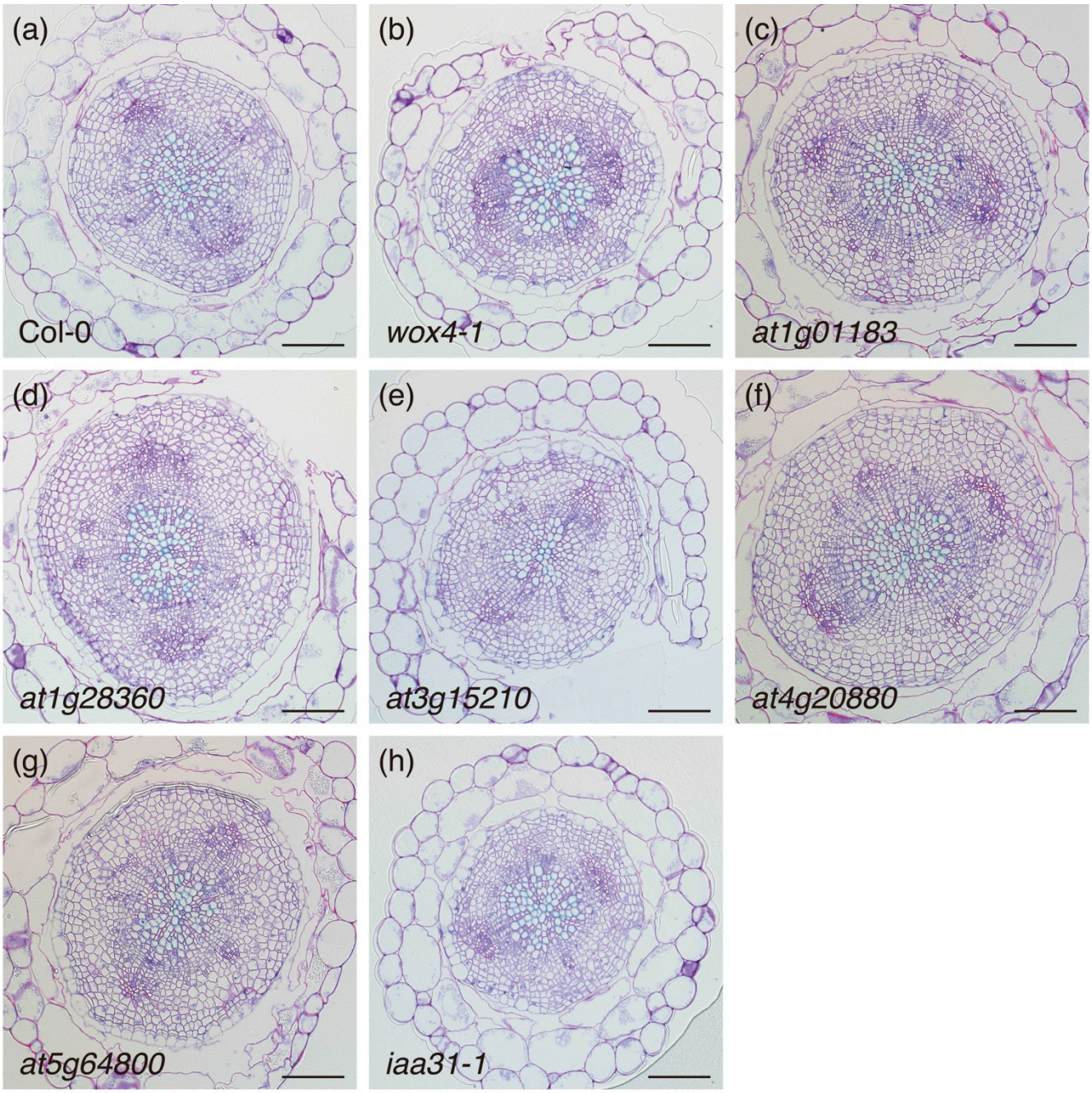

Figure 4-4. Hypocotyl sections of WOX4-related gene mutants
Seedlings were grown on 1/2 MS agar plates for 16 days.
(a) Col-0. (b) *wox4-1*. (c) *at1g01183*. (d) *at1g28360*. (e) *at3g15210*. (f) *at4g20880*. (g) *at5g64800*. (h) *iaa31-1*.
Scale bars = 100 μm.

Chapter V: Concluding remarks

In this study, I analyzed two important processes of CLE signaling pathways. One is CLE peptide processing machinery in CLE peptide-producing cells and another is downstream gene expression of a *WOX* gene that is a target of CLE signaling in CLE peptide-perceiving cells.

As regards CLE peptide processing machinery, I first demonstrated that SOL1 is a processing enzyme for CLE19 and that SOL1-dependent processing of C-terminal arginine is critical for CLE19 function. Furthermore, my biochemical experiments revealed that SOL1 possesses enzymatic activity to remove C-terminal arginine and lysine from CLE21 and CLE22 proproteins *in vitro*, suggesting involvement of SOL1 also in processing of these CLE proproteins *in planta*. Collectively, SOL1 was raised as an essential factor in CLE processing. However, comparison between CLV3 and CLE19 suggested that there are still other uncharacterized peptidases involved in CLE processing.

To understand WOX function as a target of the CLE signaling, I investigated downstream genes of both WOX4 and WUS. First, I produced transgenic *Arabidopsis* cell cultures expressing estrogen-inducible *WOX4-ECFP* and *WUS-ECFP*. Using these cultures, I performed microarray analysis and found that *WOX4-ECFP* and *WUS-ECFP* could induce the expression of a number of genes. *WOX4-ECFP*-induced genes were largely different from *WUS-ECFP*-induced genes, implying very different function between WOX4 and WUS. Detailed analysis of candidates of target genes of WOX4

including ethylene-related genes is underway.

In this study, I intended to reveal general mechanisms of CLE signaling. As a result, I indicated that SOL1 is commonly involved in processing of several CLE peptides including CLE19, CLE21 and CLE22. On the other hand, my result implied that there should be other peptidases involved in processing of CLE proproteins. The comparison between candidates of downstream genes of WOX4 and WUS indicated that most of candidate genes are different, suggesting their distinct functions. Further studies are necessary to determine other processing enzymes than SOL1 and key downstream genes both of WOX4 and WUS. These studies will provide critical insight into CLE signaling and functions.

References

Bleckmann, A., Weidtkamp-Peters, S., Seidel, C. and Simon, R. (2010) Stem cell signaling in Arabidopsis requires CRN to localize CLV2 to the plasma membrane. *Plant Physiol*. **152**, 166-176.

Boevink, P., Oparka, K., Santa Cruz, S., Martin, B., Betteridge, A. and Hawes, C. (1998) Stacks on tracks: the plant Golgi apparatus traffics on an actin/ER network. *Plant J.* **15**, 441-447.

Breuninger, H., Rikirsch, E., Hermann, M., Ueda, M. and Laux, T. (2008) Differential expression of *WOX* genes mediates apical-basal axis formation in the *Arabidopsis* embryo. *Dev. Cell*. **14**, 867-876.

Busch, W., Miotk, A., Ariel, F.D., Zhao, Z., Forner, J., Daum, G., Suzaki, T., Schuster, C., Schultheiss, S.J., Leibfried, A., Haubeiss, S., Ha, N., Chan, R.L. and Lohmann, J.U. (2010) Transcriptional control of a plant stem cell niche. *Dev. Cell*. **18**, 849-861.

Casamitjana-Martínez, E., Hofhuis, H.F., Xu, J., Liu, C.M., Heidstra, R. and Scheres, B. (2003) Root-specific *CLE19* overexpression and the *sol1/2* suppressors implicate a CLV-like pathway in the control of *Arabidopsis* root meristem maintenance. *Curr. Biol*. **13**, 1435-1441.

Clark, S.E., Running, M.P. and Meyerowitz, E.M. (1993) *CLAVATA1*, a regulator of meristem and flower development in *Arabidopsis*. *Development*, **119**, 397-418.

Clark, S.E., Running, M.P. and Meyerowitz, E.M. (1995) *CLAVATA3* is a specific regulator of shoot and floral meristem development affecting the same processes as *CLAVATA1*. *Development*, **121**, 2057-2067.

Clough, S.J. and Bent, A.F. (1998) Floral dip: a simplified method for *Agrobacterium*-mediated transformation of *Arabidopsis thaliana*. *Plant J.* **16**, 735-743.

Cock, J.M. and McCormick, S. (2001) A large family of genes that share homology with *CLAVATA3*. *Plant Physiol*. **126**, 939-942.

Curtis, M.D. and Grossniklaus, U. (2003) A gateway cloning vector set for high-throughput functional analysis of genes in planta. *Plant Physiol*. **133**, 462-469.

Davidson, H.W. (2004) (Pro)Insulin processing: a historical perspective. *Cell Biochem.*

Biophys. **40**, 143-158.

Diévart, A., Dalal, M., Tax, F.E., Lacey, A.D., Huttly, A., Li, J. and Clark, S.E. (2003) *CLAVATA1* dominant-negative alleles reveal functional overlap between multiple receptor kinases that regulate meristem and organ development. *Plant Cell*, **15**, 1198-1211.

Djordjevic, M.A., Oakes, M., Wong, C.E., Singh, M., Bhalla, P., Kusumawati, L. and Imin, N. (2011) Border sequences of *Medicago truncatula* CLE36 are specifically cleaved by endoproteases common to the extracellular fluids of *Medicago* and soybean. *J. Exp. Bot*. **62**, 4649-4659.

Docherty, K. and Hutton, J.C. (1983) Carboxypeptidase activity in the insulin secretory granule. *FEBS Lett*. **162**, 137-141.

Dong, W., Fricker, L.D. and Day, R. (1999) Carboxypeptidase D is a potential candidate to carry out redundant processing functions of carboxypeptidase E based on comparative distribution studies in the rat central nervous system. *Neuroscience*, **89**, 1301-1317.

Ebine, K., Fujimoto, M., Okatani, Y., Nishiyama, T., Goh, T., Ito, E., Dainobu, T., Nishitani, A., Uemura, T., Sato, M.H., Thordal-Christensen, H., Tsutsumi, N., Nakano, A. and Ueda, T. (2011) A membrane trafficking pathway regulated by the plant-specific RAB GTPase ARA6. *Nat. Cell. Biol*. **13**, 853-859.

Etchells, J.P., Provost, C.M. and Turner, S.R. (2012) Plant Vascular Cell Division Is Maintained by an Interaction between PXY and Ethylene Signalling. *PLoS Genet*. **8**, e1002997.

Fiers, M., Golemiec, E., van der Schors, R., van der Geest, L., Li, K.W., Stiekema, W.J. and Liu, C.M. (2006) The CLAVATA3/ESR motif of CLAVATA3 is functionally independent from the nonconserved flanking sequences. *Plant Physiol*. **141**, 1284-1292.

Fiers, M., Golemiec, E., Xu, J., van der Geest, L., Heidstra, R., Stiekema, W. and Liu, C.M. (2005) The 14-amino acid CLV3, CLE19, and CLE40 peptides trigger consumption of the root meristem in *Arabidopsis* through a *CLAVATA2*-dependent pathway. *Plant Cell*, **17**, 2542-2553.

Fricker, L.D. (1988) Carboxypeptidase E. *Annu. Rev. Physiol*. **50**, 309-321.

Fricker, L.D. and Snyder, S.H. (1983) Purification and characterization of enkephalin

convertase, an enkephalin-synthesizing carboxypeptidase. *J. Biol. Chem*. **258**, 10950-10955.

Greene, D., Das, B. and Fricker, L.D. (1992) Regulation of carboxypeptidase E. Effect of pH, temperature and Co^{2+} on kinetic parameters of substrate hydrolysis. *Biochem. J*. **285**, 613-618.

Haecker, A., Gross-Hardt, R., Geiges, B., Sarkar, A., Breuninger, H., Herrmann, M. and Laux, T. (2004) Expression dynamics of *WOX* genes mark cell fate decisions during early embryonic patterning in *Arabidopsis thaliana*. *Development*, **131**, 657-668.

Hirakawa, Y., Shinohara, H., Kondo, Y., Inoue, A., Nakanomyo, I., Ogawa, M., Sawa, S., Ohashi-Ito, K., Matsubayashi, Y. and Fukuda, H. (2008) Non-cell-autonomous control of vascular stem cell fate by a CLE peptide/receptor system. *Proc. Natl Acad. Sci. USA*, **105**, 15208-15213.

Hirakawa, Y., Kondo, Y. and Fukuda, H. (2010) TDIF peptide signaling regulates vascular stem cell proliferation via the *WOX4* homeobox gene in *Arabidopsis*. *Plant Cell*, **22**, 2618-2629.

Hirakawa, Y., Kondo, Y. and Fukuda, H. (2011) Establishment and maintenance of vascular cell communities through local signaling. *Curr. Opin. Plant Biol*. **14**, 17-23.

Hook, V.Y.H. and Loh, Y.P. (1984) Carboxypeptidase B-like converting enzyme activity in secretory granules of rat pituitary. *Proc. Natl Acad. Sci. USA*, **81**, 2776-2880.

Hoyle, D.C., Rattray, M., Jupp, R. and Brass, A. (2002) Making sense of microarray data distributions. *Bioinformatics*, **18**, 576-584.

Ikeda, M., Mitsuda, N. and Ohme-Takagi, M. (2009) *Arabidopsis* WUSCHEL is a bifunctional transcription factor that acts as a repressor in stem cell regulation and as an activator in floral patterning. *Plant Cell*, **21**, 3493-3505.

Ito, Y., Nakanomyo, I., Motose, H., Iwamoto, K., Sawa, S., Dohmae, N. and Fukuda, H. (2006) Dodeca-CLE peptides as suppressors of plant stem cell differentiation. *Science*, **313**, 842-845.

Jun, J., Fiume, E., Roeder, A.H., Meng, L., Sharma, V.K., Osmont, K.S., Baker, C., Ha, C.M., Meyerowitz, E.M., Feldman, L.J. and Fletcher, J.C. (2010) Comprehensive analysis of *CLE* polypeptide signaling gene expression and

overexpression activity in Arabidopsis. *Plant Physiol*. **154**, 1721-1736.

Kayes, J.M. and Clark, S.E. (1998) *CLAVATA2*, a regulator of meristem and organ development in *Arabidopsis*. *Development*, **125**, 3843-3851.

Kinoshita, A., Betsuyaku, S., Osakabe, Y., Mizuno, S., Nagawa, S., Stahl, Y., Simon, R., Yamaguchi-Shinozaki, K., Fukuda, H. and Sawa, S. (2010) RPK2 is an essential receptor-like kinase that transmits the CLV3 signal in *Arabidopsis*. *Development*, **137**, 3911-3920.

Kinoshita, A., Nakamura, Y., Sasaki, E., Kyozuka, J., Fukuda, H. and Sawa, S. (2007) Gain-of-function phenotypes of chemically synthetic CLAVATA3/ESR-related (CLE) peptides in *Arabidopsis thaliana* and *Oryza sativa*. *Plant Cell Physiol*. **48**, 1821-1825.

Kiyohara, S. and Sawa, S. (2012) CLE signaling systems during plant development and nematode infection. *Plant Cell Physiol*. **53**, 1989-1999.

Kleinboelting, N., Huep, G., Kloetgen, A., Viehoever, P. and Weisshaar, B. (2012) GABI-Kat SimpleSearch: new features of the Arabidopsis thaliana T-DNA mutant database. *Nucleic Acids Res*. **40**, D1211-1215.

Kondo, T., Sawa, S., Kinoshita, A., Mizuno, S., Kakimoto, T., Fukuda, H. and Sakagami, Y. (2006) A plant peptide encoded by *CLV3* identified by in situ MALDI-TOF MS analysis. *Science*, **313**, 845-848.

Kondo, T., Kajita, R., Miyazaki, A., Hokoyama, M., Nakamura-Miura, T., Mizuno, S., Masuda, Y., Irie, K., Tanaka, Y., Takada, S., Kakimoto, T. and Sakagami, Y. (2010) Stomatal density is controlled by a mesophyll-derived signaling molecule. *Plant Cell Physiol*. **51**, 1-8.

Kondo, Y., Hirakawa, Y., Kieber, J.J. and Fukuda, H. (2011) CLE peptides can negatively regulate protoxylem vessel formation via cytokinin signaling. *Plant Cell Physiol*. **52**, 37-48.

Kotzer, A.M., Brandizzi, F., Neumann, U., Paris, N., Moore, I. and Hawes, C. (2004) AtRabF2b (Ara7) acts on the vacuolar trafficking pathway in tobacco leaf epidermal cells. *J. Cell Sci*. **117**, 6377-6389.

Leibfried, A., To, J.P., Busch, W., Stehling, S., Kehle, A., Demar, M., Kieber, J.J. and Lohmann, J.U. (2005) WUSCHEL controls meristem function by direct regulation of cytokinin-inducible response regulators. *Nature*, **438**, 1172-1175.

Lohmann, J.U., Hong, R.L., Hobe, M., Busch, M.A., Parcy, F., Simon, R. and

Weigel, D. (2001) A molecular link between stem cell regulation and floral patterning in *Arabidopsis*. *Cell*, **105**, 793-803.

Love, J., Bjorklund, S., Vahala, J., Hertzberg, M., Kangasjarvi, J. and Sundberg, B. (2009) Ethylene is an endogenous stimulator of cell division in the cambial meristem of *Populus*. *Proc. Natl Acad. Sci. USA*, **106**, 5984-5989.

Mathur, J., Szabados, L., Schaefer, S., Grunenberg, B., Lossow, A., Jonas-Straube, E., Schell, J., Koncz, C. and Koncz-Kalman, Z. (1998) Gene identification with sequenced T-DNA tags generated by transformation of *Arabidopsis* cell suspension. *Plant J.* **13**, 707-716.

Matsubayashi, Y. (2011) Small Post-Translationally Modified Peptide Signals in Arabidopsis. *The Arabidopsis Book*, **9**, e0150.

Matsuzaki, Y., Ogawa-Ohnishi, M., Mori, A. and Matsubayashi, Y. (2010) Secreted peptide signals required for maintenance of root stem cell niche in *Arabidopsis*. *Science*, **329**, 1065-1067.

Mitsuhashi, N., Shimada, T., Mano, S., Nishimura, M. and Hara-Nishimura, I. (2000) Characterization of Organelles in the Vacuolar-Sorting Pathway by Visualization with GFP in Tobacco BY-2 Cells. *Plant Cell Physiol*. **41**, 993-1001.

Miwa, H., Betsuyaku, S., Iwamoto, K., Kinoshita, A., Fukuda, H. and Sawa, S. (2008) The receptor-like kinase SOL2 mediates CLE signaling in *Arabidopsis*. *Plant Cell Physiol*. **49**, 1752-1757.

Mizuno, S., Osakabe, Y., Maruyama, K., Ito, T., Osakabe, K., Sato, T., Shinozaki, K. and Yamaguchi-Shinozaki, K. (2007) Receptor-like protein kinase 2 (RPK 2) is a novel factor controlling anther development in *Arabidopsis thaliana*. *Plant J*. **50**, 751-766.

Moubayidin, L., Di Mambro, R. and Sabatini, S. (2009) Cytokinin-auxin crosstalk. *Trends Plant Sci.* **14**, 557-562.

Muller, L., Zhu, P., Juliano, M.A., Juliano, L. and Lindberg, I. (1999) A 36-Residue Peptide Contains All of the Information Required for 7B2-mediated Activation of Prohormone Convertase 2. *J. Biol. Chem.* **274**, 21471-21477.

Müller, R., Bleckmann, A. and Simon, R. (2008) The receptor kinase CORYNE of *Arabidopsis* transmits the stem cell-limiting signal CLAVATA3 independently of CLAVATA1. *Plant Cell*, **20**, 934-946.

Nakata, M., Matsumoto, N., Tsugeki, R., Rikirsch, E., Laux, T. and Okada, K. (2012) Roles of the middle domain-specific *WUSCHEL-RELATED HOMEOBOX* genes in early development of leaves in *Arabidopsis*. *Plant Cell*, **24**, 519-535.

Ni, J. and Clark, S.E. (2006) Evidence for functional conservation, sufficiency, and proteolytic processing of the CLAVATA3 CLE domain. *Plant Physiol*. **140**, 726-733.

Ni, J., Guo, Y., Jin, H., Hartsell, J. and Clark, S.E. (2011) Characterization of a CLE processing activity. *Plant Mol. Biol*. **75**, 67-75.

Oda, Y., Iida, Y., Kondo, Y. and Fukuda, H. (2010) Wood cell-wall structure requires local 2D-microtubule disassembly by a novel plasma membrane-anchored protein. *Curr. Biol*. **20**, 1197-1202.

Oelkers, K., Goffard, N., Weiller, G.F., Gresshoff, P.M., Mathesius, U. and Frickey, T. (2008) Bioinformatic analysis of the CLE signaling peptide family. *BMC Plant Biol*. **8**, 1.

Ogawa, M., Shinohara, H., Sakagami, Y. and Matsubayashi, Y. (2008) *Arabidopsis* CLV3 peptide directly binds CLV1 ectodomain. *Science*, **319**, 294.

Ohashi-Ito, K., Oda, Y. and Fukuda, H. (2010) *Arabidopsis* VASCULAR-RELATED NAC-DOMAIN6 directly regulates the genes that govern programmed cell death and secondary wall formation during xylem differentiation. *Plant Cell*, **22**, 3461-3473.

Ohyama, K., Ogawa, M. and Matsubayashi, Y. (2008) Identification of a biologically active, small, secreted peptide in Arabidopsis by *in silico* gene screening, followed by LC-MS-based structure analysis. *Plant J*. **55**, 152-160.

Ohyama, K., Shinohara, H., Ogawa-Ohnishi, M. and Matsubayashi, Y. (2009) A glycopeptide regulating stem cell fate in *Arabidopsis thaliana*. *Nat. Chem. Biol*. **5**, 578-580.

Okuda, S., Tsutsui, H., Shiina, K., Sprunck, S., Takeuchi, H., Yui, R., Kasahara, R.D., Hamamura, Y., Mizukami, A., Susaki, D., Kawano, N., Sakakibara, T., Namiki, S., Itoh, K., Otsuka, K., Matsuzaki, M., Nozaki, H., Kuroiwa, T., Nakano, A., Kanaoka, M.M., Dresselhaus, T., Sasaki, N. and Higashiyama, T. (2009) Defensin-like polypeptide LUREs are pollen tube attractants secreted from synergid cells. *Nature*, **458**, 357-361.

Olsen, A.N. and Skriver, K. (2003) Ligand mimicry? Plant-parasitic nematode polypeptide with similarity to CLAVATA3. *Trends Plant Sci*. **8**, 55-57.

Pearce, G., Moura, D.S., Stratmann, J. and Ryan, C.A. (2001) RALF, a 5-kDa ubiquitous polypeptide in plants, arrests root growth and development. *Proc. Natl Acad. Sci. USA*, **98**, 12843-12847.

Rojo, E., Sharma, V.K., Kovaleva, V., Raikhel, N.V. and Fletcher, J.C. (2002) CLV3 is localized to the extracellular space, where it activates the Arabidopsis CLAVATA stem cell signaling pathway. *Plant Cell*, **14**, 969-977.

Sanderfoot, A.A., Kovaleva, V., Bassham, D.C. and Raikhel, N.V. (2001) Interactions between syntaxins identify at least five SNARE complexes within the Golgi/prevacuolar system of the Arabidopsis cell. *Mol. Biol. Cell*, **12**, 3733-3743.

Sidyelyeva, G. and Fricker, L.D. (2002) Characterization of *Drosophila* carboxypeptidase D. *J. Biol. Chem*. **277**, 49613-49620.

Sohn, E.J., Kim, E.S., Zhao, M., Kim, S.J., Kim, H., Kim, Y.W., Lee, Y.J., Hillmer, S., Sohn, U., Jiang, L. and Hwang, I. (2003) Rha1, an Arabidopsis Rab5 homolog, plays a critical role in the vacuolar trafficking of soluble cargo proteins. *Plant Cell*, **15**, 1057-1070.

Srivastava, R., Liu, J.X., Guo, H.Q., Yin, Y.H. and Howell, S.H. (2009) Regulation and processing of a plant peptide hormone, AtRALF23, in Arabidopsis. *Plant J.* **59**, 930-939.

Srivastava, R., Liu, J.X. and Howell, S.H. (2008) Proteolytic processing of a precursor protein for a growth-promoting peptide by a subtilisin serine protease in Arabidopsis. *Plant J*. **56**, 219-227.

Stahl, Y., Wink, R.H., Ingram, G.C. and Simon, R. (2009) A signaling module controlling the stem cell niche in *Arabidopsis* root meristems. *Curr. Biol*. **19**, 909-914.

Ueda, T., Yamaguchi, M., Uchimiya, H. and Nakano, A. (2001) Ara6, a plant-unique novel type Rab GTPase, functions in the endocytic pathway of *Arabidopsis thaliana*. *EMBO J*. **20**, 4730-4741.

Uemura, T., Ueda, T., Ohniwa, R.L., Nakano, A., Takeyasu, K. and Sato, M.H. (2004) Systematic analysis of SNARE molecules in *Arabidopsis*: dissection of the post-Golgi network in plant cells. *Cell Struct. Funct*. **29**, 49-65.

Vandenbussche, M., Horstman, A., Zethof, J., Koes, R., Rijpkema, A.S. and Gerats, T. (2009) Differential recruitment of WOX transcription factors for lateral development and organ fusion in Petunia and *Arabidopsis*. *Plant Cell*, **21**, 2269-2283.

Varlamov, O., Eng, F.J., Novikova, E.G. and Fricker, L.D. (1999) Localization of metallocarboxypeptidase D in AtT-20 cells. Potential role in prohormone processing. *J. Biol. Chem*. **274**, 14759-14767.

Varlamov, O. and Fricker, L.D. (1998) Intracellular trafficking of metallocarboxypeptidase D in AtT-20 cells: Localization to the trans-Golgi network and recycling from the cell surface. *J. Cell Sci.* **111**, 877-885.

Varlamov, O., Fricker, L.D., Furukawa, H., Steiner, D.F., Langley, S.H. and Leiter, E.H. (1997) β-cell lines derived from transgenic Cpe^{fat}/Cpe^{fat} mice are defective in carboxypeptidase E and proinsulin processing. *Endocrinology*, **138**, 4883-4892.

Voinnet, O., Rivas, S., Mestre, P. and Baulcombe, D. (2003) An enhanced transient expression system in plants based on suppression of gene silencing by the p19 protein of tomato bushy stunt virus. *Plant J*. **33**, 949-956.

Wang, X., Kota, U., He, K., Blackburn, K., Li, J., Goshe, M.B., Huber, S.C. and Clouse, S.D. (2008) Sequential transphosphorylation of the BRI1/BAK1 receptor kinase complex impacts early events in brassinosteroid signaling. *Dev. Cell*, **15**, 220-235.

Westphal, C.H., Muller, L., Zhou, A., Zhu, X., Bonner-Weir, S., Schambelan, M., Steiner, D.F., Lindberg, I. and Leder, P. (1999) The Neuroendocrine Protein 7B2 Is Required for Peptide Hormone Processing In Vivo and Provides a Novel Mechanism for Pituitary Cushing's Disease. *Cell*, **96**, 689-700.

Yadav, R.K., Tavakkoli, M. and Reddy, G.V. (2010) WUSCHEL mediates stem cell homeostasis by regulating stem cell number and patterns of cell division and differentiation of stem cell progenitors. *Development*, **137**, 3581-3589.

Yamada, M. and Sawa, S. (2013) The roles of peptide hormones during plant root development. *Curr. Opin. Plant Biol*. **16**, 56-61.

Zuo, J., Niu, Q.W. and Chua, N.H. (2000) Technical advance: An estrogen receptor-based transactivator XVE mediates highly inducible gene expression in transgenic plants. *Plant J*. **24**, 265-273.